N71-25503

NASA CR-72852

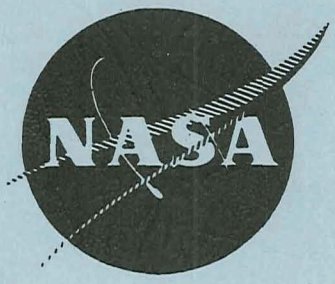

ADVANCED SUPERALLOY PROTECTION SYSTEMS EVALUATION

by

R. K. Betts and T. J. McCauley

GENERAL ELECTRIC COMPANY

prepared for

NATIONAL AERONAUTICS AND SPACE ADMINISTRATION

NASA-Lewis Research Center

Contract NAS 3-12414

F. Harf, S. J. Grisaffe, and J. P. Merutka, Project Managers

Requests for copies of this report should be referred to:

National Aeronautics and Space Administration
Office of Scientific and Technical Information
Attention: AFSS-A
Washington, D.C. 20546

ABSTRACT

Metalliding parameters were developed for the sequential deposition of Mn + Cr, Al + Y and Ta + Al to NASA/TRW VI-A alloy. Efforts to deposit Cr + Y and Y + Zr by metalliding were unsuccessful. None of the applied systems exhibited good ballistic impact resistance. The 2000°F (1367°K) oxidation resistance (dynamic or static) of all metallided systems studied was below that of conventional CODEP-type pack aluminide coating on superalloys.

Surface alloying by metalliding did not even closely appear to synthenize the structures or chemical distribution of the bulk alloys on which coating design principles were based. Straight aluminiding was the exception.

TABLE OF CONTENTS

LIST OF ILLUSTRATIONS

LIST OF ILLUSTRATIONS (Cont'd)

LIST OF ILLUSTRATIONS (Cont'd)

LIST OF ILLUSTRATIONS (Concl'd)

LIST OF TABLES

1.0 SUMMARY

Metallided sequentially deposited dual-element coating systems were investigated for 2000°F (1367°K) oxidation protection of NASA/TRW VI-A. Parameters for sequential deposition of the systems Mn + Cr, Al + Y and Ta + Al were developed. The systems Y + Cr, Y + Al and Y + Zr were not successfully metallided. Unsuccessful metalliding was largely due to loss of Y through reaction with the bath during deposition of the second element. Al was also evaluated as a metallided coating on NASA/TRW VI-A and as a CODEP coating on IN-100.

The successfully metallided coatings were ballistically impacted for adherence evaluation at room temperature and at 1900°F (1312°K). All the metallided coatings except Mn + Cr spalled when impacted at room temperature. None spalled at elevated temperature.

During 2000°F (1367°K) static oxidation tests the Mn + Cr and Ta + Al systems failed by spalling in 20 hours. The Al + Y system failed after shedding the oxidized Y-rich layer. However, the Al metallided coating showed only small weight losses during the 200-hour exposure.

In dynamic oxidation at 2000°F (1367°K) the Mn + Cr system also failed quickly but the Ta + Al system exhibited a less drastic weight loss. The Al + Y system behaved as in the static oxidation tests. CODEP aluminized coating on IN-100 was stable to nearly 600 hours but then failed rapidly.

This investigation did not produce metallided coatings which resulted in an improvement over present NiAl coating technology.

2.0 INTRODUCTION

There is a continuing need to develop an improved protection system for nickel-base turbine alloys. The objective of this program was to determine if protection systems other than conventional nickel aluminide type could be developed by sequential metallide deposition of elements other than, or in addition to, aluminum. The alloy chosen as the substrate was NASA/TRW VI-A - one of the highest strength cast nickel-base alloys yet developed. Metalliding (a G.E. development) is an electrolytic fused salt process for metal surface conversion by inward diffusion of a suitable additive metal to achieve a desired surface property such as oxidation resistance. Five coating systems were initially selected for this program.

Systems selected initially were:

1. Mn + Cr
2. Y + Cr
3. Y + Al (later reversed in order)
4. Ta + Al
5. Y + Zr

Reactive elements, specifically manganese and chromium, were chosen for System 1 on the basis of work indicating that approximately 1% manganese added to nickel-base alloys inhibits the volatilization of CrO_3 by forming $MnCr_2O_4$, a stable oxide spinel. The addition of chromium to the manganided substrate alloy was expected to produce a surface alloy favorable to forming this spinel.

For System 2, studies of rare-earth additions to nickel-chromium alloys indicate that Y can render the alloy less susceptible to oxidation. If NASA/TRW VI-A were yttrided and then chromided, a coating was expected containing Ni and Cr and stabilized by the presence of Y.

The basis for System 3 was the performance of pack or slurry-aluminided coatings currently used for nickel-base superalloys. The protective oxide has been shown to be Al_2O_3. However, less protective Ni_3Al is slowly formed by Al depletion, thus allowing oxide penetration through Ni_3Al paths. Addition of Y was expected to stabilize a NiAl coating by tying up more of the nickel and, also, by forming the more stable oxide combination of $NiAl_2O_4$ plus Al_2O_3.

Tantaliding of NASA/TRW VI-A had not been performed as of the beginning of this contract. Due to the fact that NASA/TRW VI-A already has 9% tantalum plus the high concentration of refractory elements, high coulombic

efficiencies in the tantaliding were not expected. However, other studies have produced peak concentrations of as high as 70% with a steep concentration gradient between base metal and coating. After the application of tantalum, aluminiding was expected to produce a well-bonded $TaAl_3$ outer layer, which could protect the alloy from oxidation.

It is known that stabilized zirconia is highly oxidation resistant. To apply the zirconium to the alloy, the part was first to be yttrided to a depth of 2-3 mils and then zirconided. It was anticipated that the yttrium oxide would stabilize the zirconia.

While the primary metallides had been applied to many metals and alloys other than NASA/TRW VI-A, little difference was expected other than longer times and lower efficiencies. The real development involved the application of the secondary metallide coatings to the primary coatings.

All sequentially deposited dual-element systems were selected with the intention of:

1. Producing an oxide other than Al_2O_3
2. Enriching the surface with Al and then stabilizing the subsequent Al_2O_3 with an additive
3. Beneficially alloying the Ni and stabilizing it with a second element

Metalliding process parameters for these systems were developed. The coatings produced by these selected parameters were evaluated by ballistic impact and static and dynamic oxidation at 2000°F (1367°K). The as-coated and tested systems were also analyzed by metallography and electron microprobe.

3.0 TECHNICAL PROGRAM

3.1 METALLIDING PARAMETER DEVELOPMENT

3.1.1 Metalliding Process

Metalliding is a proprietary and patented metal surface conversion process developed at the General Electric Company. The process incorporates fused salt electrolytic methods for the conversion of certain metal surfaces to obtain desirable properties. Whereas most electrolytic and thermal-spray coating procedures superimpose a metal onto a substrate, the metalliding processes like vapor or molten metal dipping can form integrally-diffused metal or intermetallics composites upon a substrate metal. Uniformity and adherence are general characteristics of metallided coatings which are also intended to have other design features such as oxidation and wear resistance.

Metalliding is accomplished by immersing the selected metallic substrate and metalliding metal in a very high purity fused salt bath composed of eutectic alkali metal fluorides and the fluoride of the metal to be deposited by metalliding. The bath temperature needs to be high enough to promote diffusion. The metalliding metal is also present as an anode which, when electrically activated, dissolves into the bath. Ions of the metal discharge at the substrate metal cathode.

The process at a given EMF is self-regulating in that the deposition rate equals the diffusion rate of the metal into the cathodic substrate. The principal parameters influencing deposition rates are the bath temperature, current density, activity in the bath, and diffusion alloying relationship of the metallide metal with the substrate.

Process limitations are such that only substrate metals higher in the electromotive series may be metallided by a lower metal. Furthermore, the salt bath temperatures required for diffusion may produce undesirable alloy property changes and low melting eutectics in the substrate.

Figure 1 illustrates a bank of metalliding reaction cells. The ceramic tubes are accesses for the anode and cathode metals, permitting cooling and purging with inert gas. Figure 2 is a schematic illustration of the metalliding electrical circuit.

3.1.2 Specimens - Alloys

Cast nickel-base alloy specimens used in this program consisted of two types:

Type A - Coupons, 1 x 2 x 0.10 inch (25.4 x 50.8 x 2.54 mm)

Type B - Paddles, conventional 1 x 2 inch (25.4 x 50.8 mm) pseudo-airfoils with stems

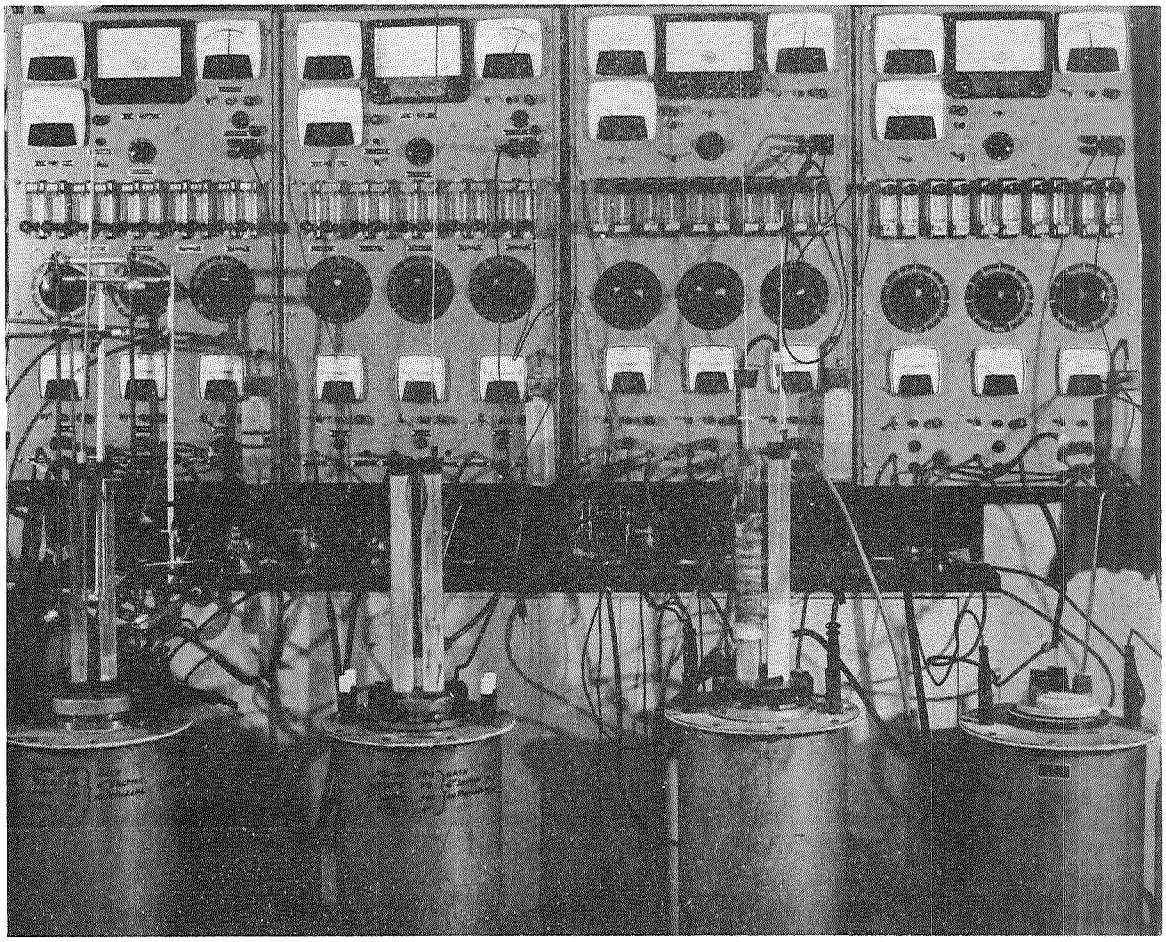

Figure 1. Metalliding Cells and Facility Typical of Those Used for the Reported Program.

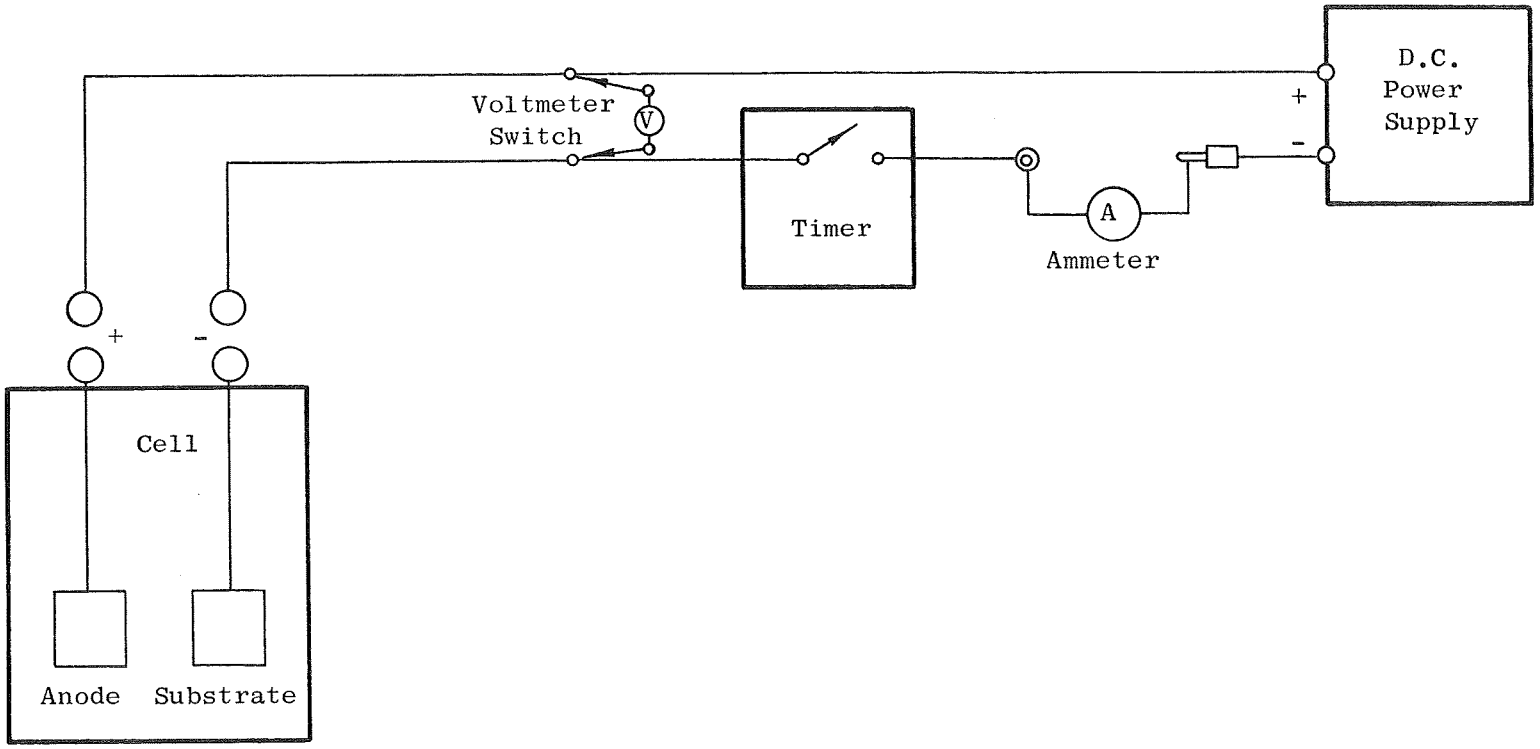

Figure 2. Metalliding Schematic Diagram.

The substrate alloy was cast NASA/TRW VI-A, having the nominal composition listed in Table I. IN-100 Alloy was also the substrate for a comparative coating system.

Table I. Substrate Alloy Nominal Composition - w/o.

Material	NASA/TRW VI-A	IN-100
Ni	61.5	60.0
Ta	9.0	---
Co	7.5	15.0
Cr	6.0	9.5
W	6.0	---
Al	5.5	5.5
Mo	2.0	3.0
Ti	1.0	4.2
Cb	0.5	Fe 1.0
Re	0.4	V 1.0
Hf	0.4	Mn 0.5
Si	---	0.5
Zr	0.1	0.06
C	0.14	0.18
B	0.02	0.02

3.1.3 Mn + Cr, System 1

Manganiding the NASA/TRW VI-A alloy consistently resulted in high coulombic efficiency. That is, the EMF potential between the Mn and substrate was sufficiently high to enable relatively rapid deposition rates. Figure 3 illustrates the manganided layer. Note the presence of fine cracks.

Suitable chromiding required considerable experimentation. Examination of the microstructures after chromiding revealed voids in the Mn-rich layer and the diffusion zone between the Mn and Cr layers, as shown in Figure 4. The specimens were then given a heat treatment at 2200°F (1478°K) for 1 hour in vacuum. Diffusion broadened the general coating layer, and some additional voids appeared in the outward Cr-rich layer. No voids were visible in the newly-formed innermost diffusion zone.

While manganiding at 1800°F (1258°K) resulted in subsequent chromiding with higher Cr than planned (10 to 25%), it represented the most repeatable process conditions and the only one to result in a smooth chromium layer after chromiding. The recommended manganiding/chromiding parameters are given in Table II, and a microphotograph of the recommended coating is presented in Figure 4.

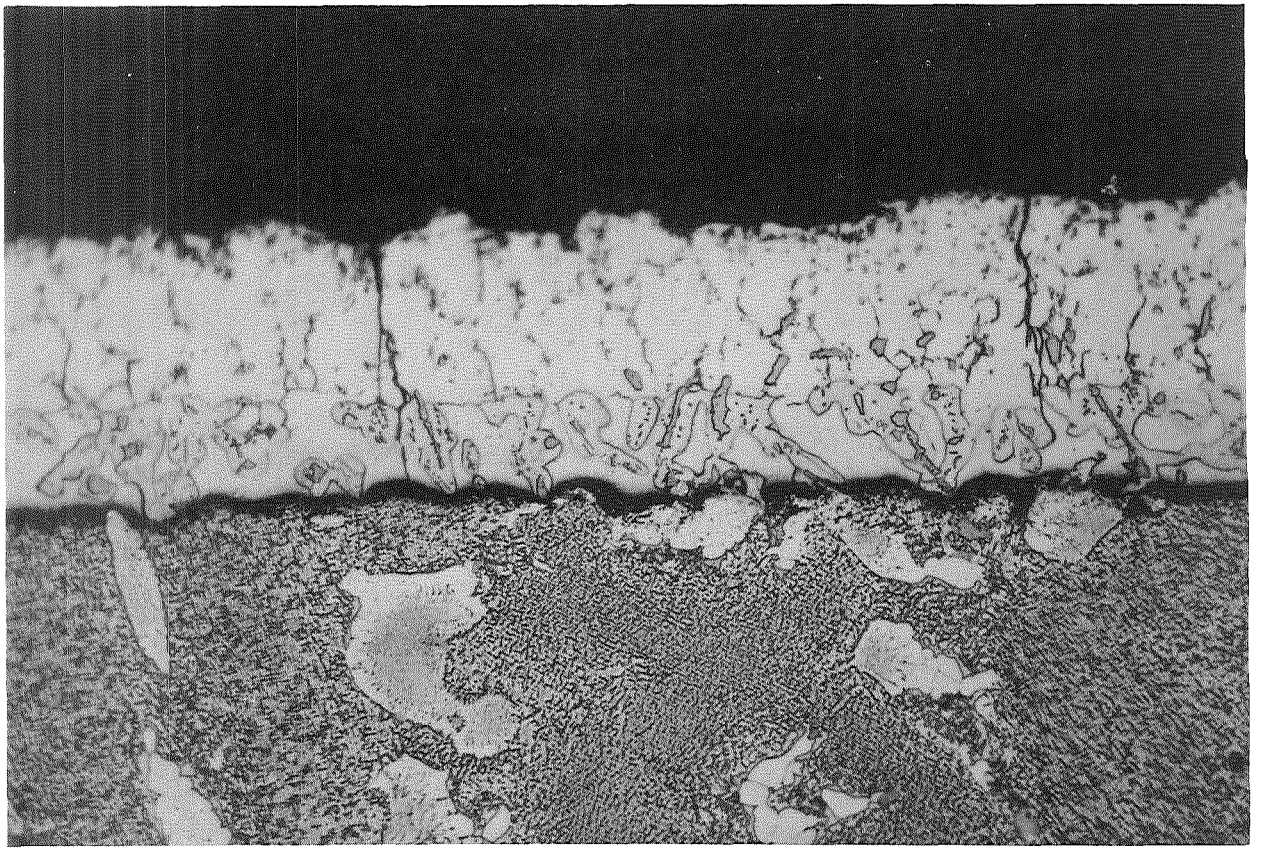

Figure 3. Manganided Surface of NASA/TRW VI-A Alloy As-Processed (Neg. B 7555, Mount A 7771, 500X, TRW Etch*).

*Etchant for NASA/TRW VI-A Alloy

160 ml H_3PO_4

5 ml H_2SO_4

30 ml CH_3COOH

50 ml H_2O

Electrolytic, 5v

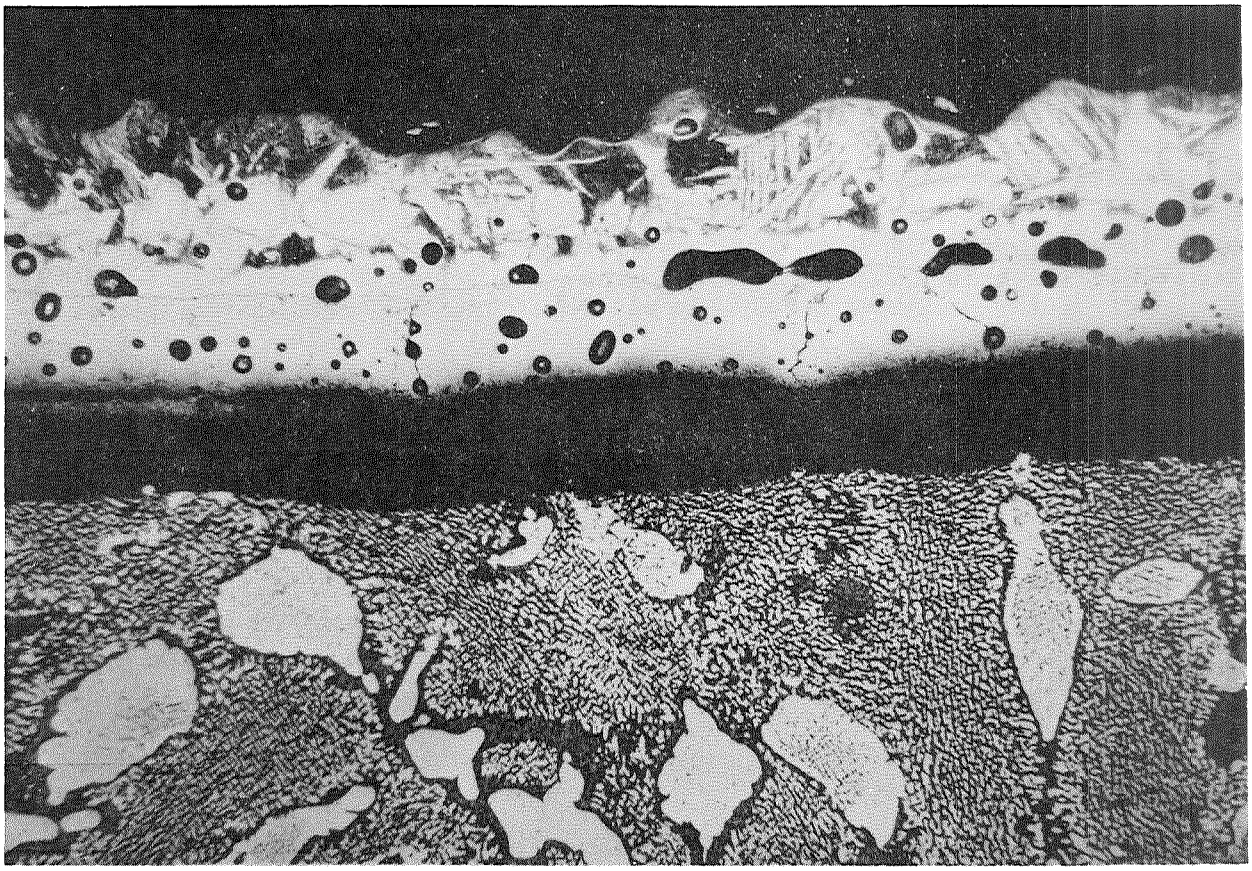

Figure 4. Manganided/Chromided System As-Processed (Neg. B 10322, Mount A 11107, 500X, TRW Etch).

Table II. Selected Parameters for Manganiding/Chromiding.

Process Step	Operation	Temperature, °F (°K)	Current Density, ma/cm^2	Time, Hrs	Bath Composition*
1	Manganide	1800 (1258)	2	5	0.3 MnF_2
2	Chromide	1900 (1310)	2	24	0.3 CrF_2
3	Vacuum Treat	2200 (1478)	---	1	---

*Mol % in LiF

Formation of the Mn + Cr systems was slower than encountered in other known metalliding processes because of slower diffusion of the coating elements into the NASA/TRW VI-A substrate. While the manganiding efficiency (actual weight gain/calculated weight gain) was generally excellent (95-100%), the subsequent chromiding efficiency was low. The long metalliding time required for Cr allowed significant loss of Mn by dissolution, resulting in low residual concentration in the coating. Furthermore, contamination of the chromiding salt by Mn further hampered its efficiency. Mn dissolved into the bath because its affinity for the fluoride ion was higher than that of Cr. Figure 5 is a microprobe analysis of the system showing the low residual Mn and a peak of 45% Cr in the outer 1-mil layer.

3.1.4 Y + Cr, System 2

Attempts to form this metallided system were unsuccessful due to the difficulty in retaining yttrium at the alloy surface. Three limiting factors encountered in yttriding were:

1. Y applied directly and rapidly to the substrate formed a low-melting Y-Ni eutectic.

2. Slow deposition rates allowed the Y anode to dissolve in the bath and alter the lithium fluoride salt bath composition.

3. Oxidation of the Y anode in impure cover gas resulted in rapid dissolution of Y_2O_3 into the bath and displacement of Li out of the bath as a vapor.

The upper limits of the time-and-current-density parameters were determined by the formation of the Y-Ni eutectic, which melts at 1475°F (1072°K). Figure 6 illustrates a microstructure of the brittle yttrided substrate.

Subsequent chromiding was largely unsuccessful because of the slow rate of Cr deposition. During chromiding, the Y would dissolve. Microprobe scanning of six specimens revealed no significant Y after chromiding.

The oxygen contamination problem was eventually eliminated by passing the argon cover gas through Ti chips at 600°C (873°K) and wrapping the Y anode in perforated Ta foil.

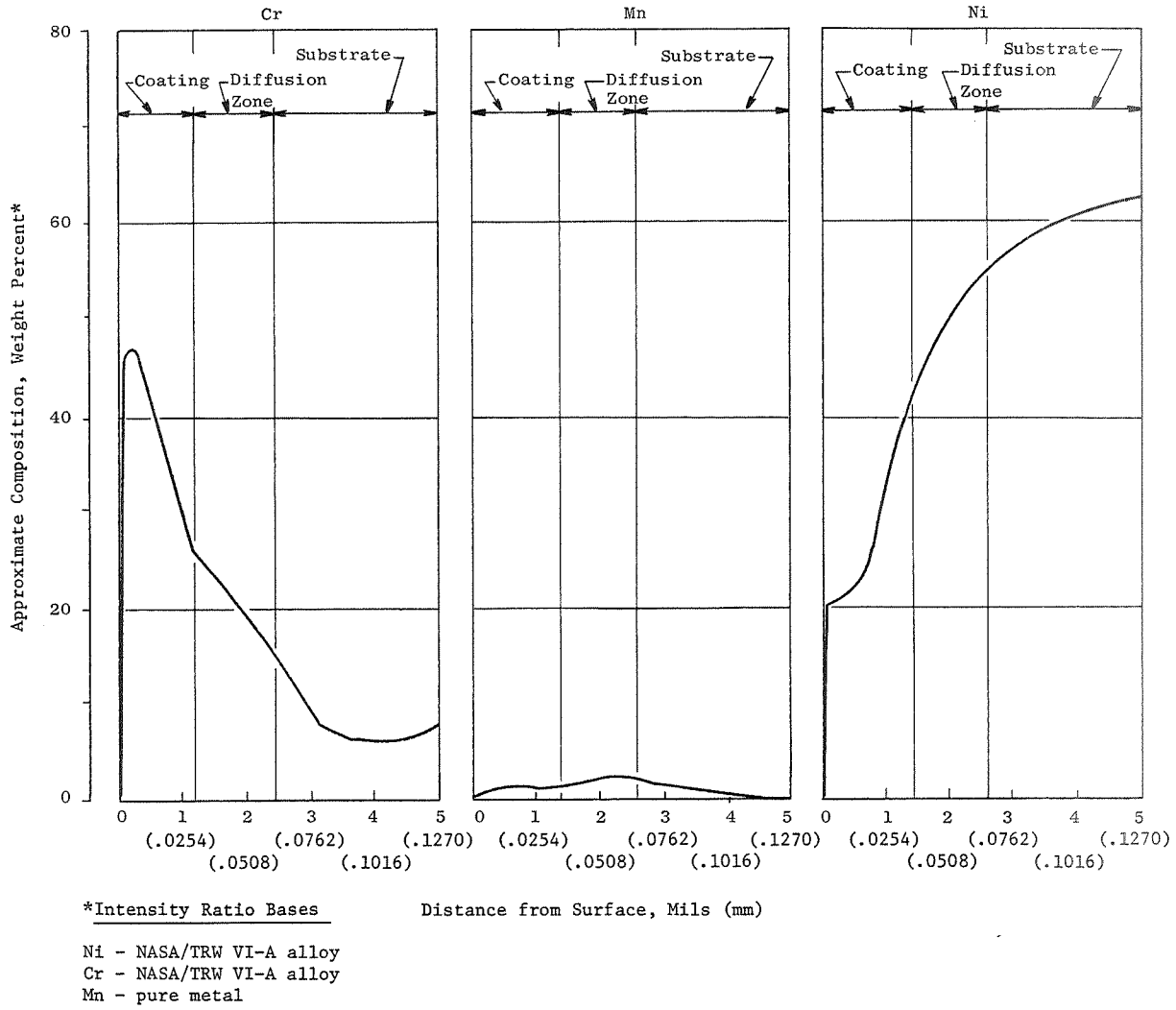

Figure 5. Microanalysis of Metallided Mn + Cr System on NASA/TRW VI-A.

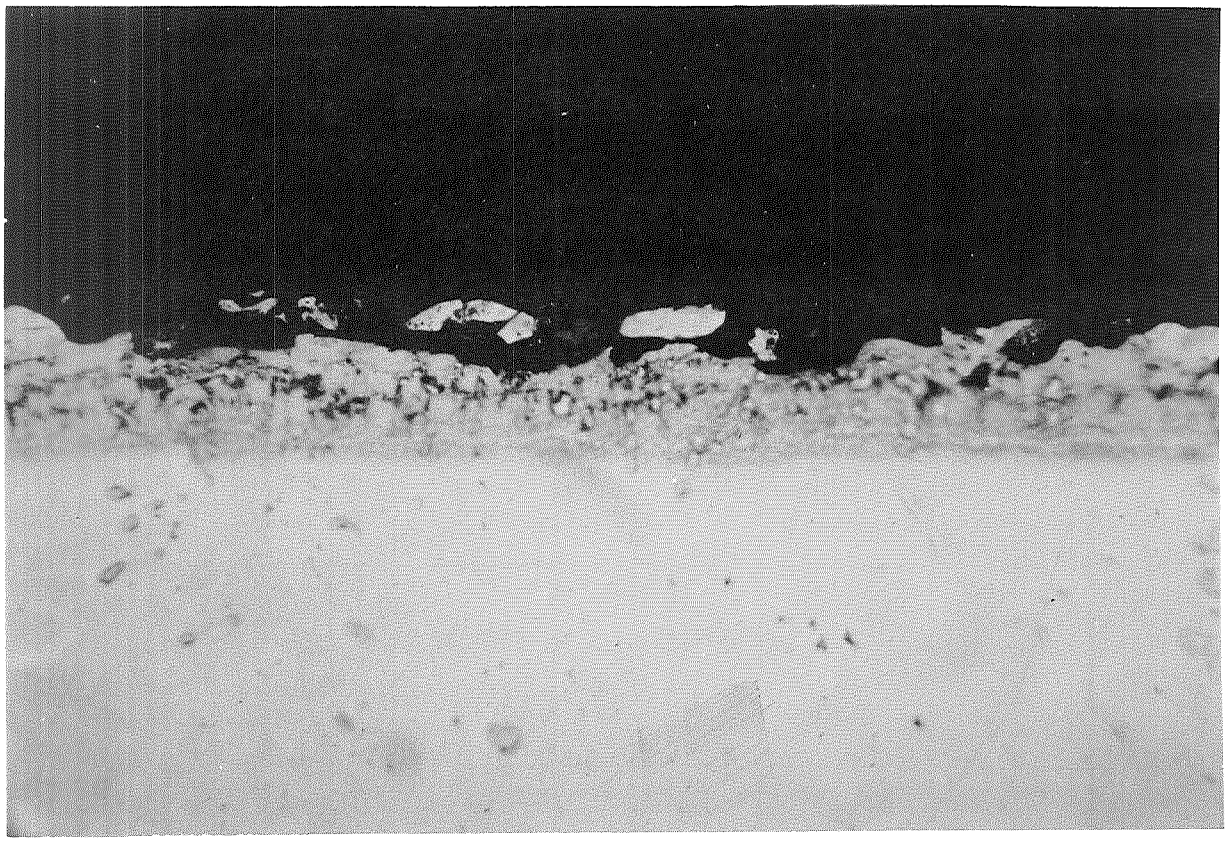

Figure 6. Yttrided Surface of NASA/TRW VI-A Alloy As-Processed (Neg. B 7876, Mount A 8048, 500X, Unetched).

In another attempt to produce the desired Y-stabilized Ni-Cr system, the Cr was applied first; but, subsequent yttriding was ineffective because of the extremely low rate of Y diffusion in Cr at the bath temperature range used. Consequently, the Y-Cr system was discarded.

3.1.5 Al + Y, System 3

This system was originally proposed as Y + Al; however, the preceding work with System 2 showed that Y applied first would subsequently redissolve, thus the order of metalliding was reversed. Deposition of Al on the alloy was accomplished with relative ease, at 100% coulombic efficiency and in short times. The most uniform aluminided coatings were produced with the highest current densities investigated.

Yttriding of the aluminided specimens was performed using the oxygen-removal techniques developed for the Y + Cr system. Deposition rates were rapid, but efficiency was generally only 20-30%. Table III lists the selected development parameters.

Table III. Selected Parameters for Aluminiding/Yttriding.

Process Step	Operation	Temperature, °F	(°K)	Current Density, ma/cm^2	Time, Hrs	Bath Composition*
1	Aluminide	1800	(1258)	6	8	0.3 AlF_3
2	Yttride	1750	(1232)	6	2	0.3 YF_3
3	Vacuum Treat	2200	(1478)	---	1	---

*Mol % in LiF

Figure 7 illustrates the microstructure of an as-coated specimen produced by the selected parameters.

Figure 8 is an electron microprobe trace of the specimen. It shows the thicker grey band of the microstructure to be the primary diffusion layer of Al into the alloy. The thin outer layer contains principally Al and Y with Ni diminishing from 45% to zero. No more than 50-60% Y was detected and only in the outer 1/2 mil (0.0127 mm).

3.1.6 Ta + Al, System 4

Initial attempts to tantalide produced very thin coatings, even using parameters which involved very long processing time at low current density. The tantaliding generally produced inconsistent results. Oxygen contamination of the bath appeared to be a significant factor. Coating efficiencies were moderately low and adherence was also a problem. Using an effective gettering technique, a series of specimens was eventually tantalided with those conditions and then aluminided.

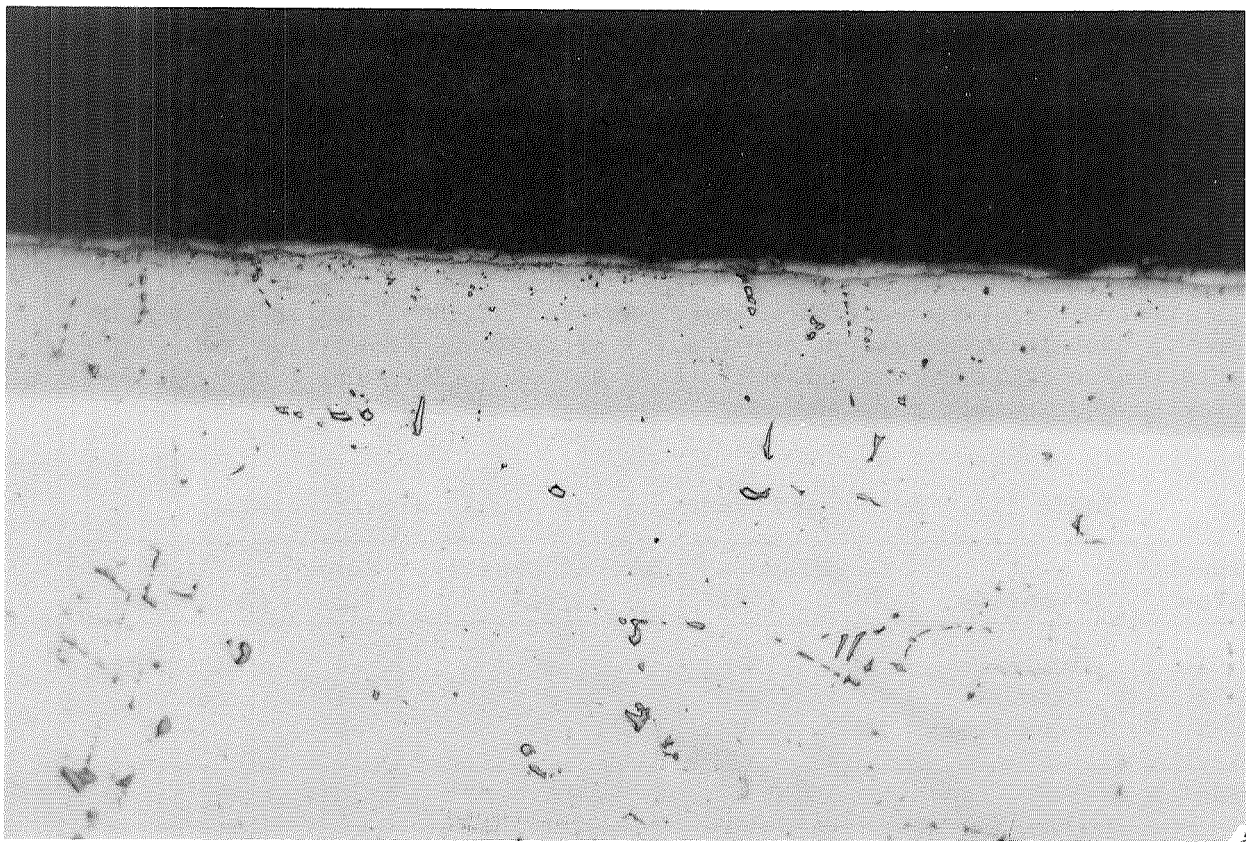

Figure 7. Aluminided/Yttrided System As-Processed (Neg. B 11341, 250X, Unetched).

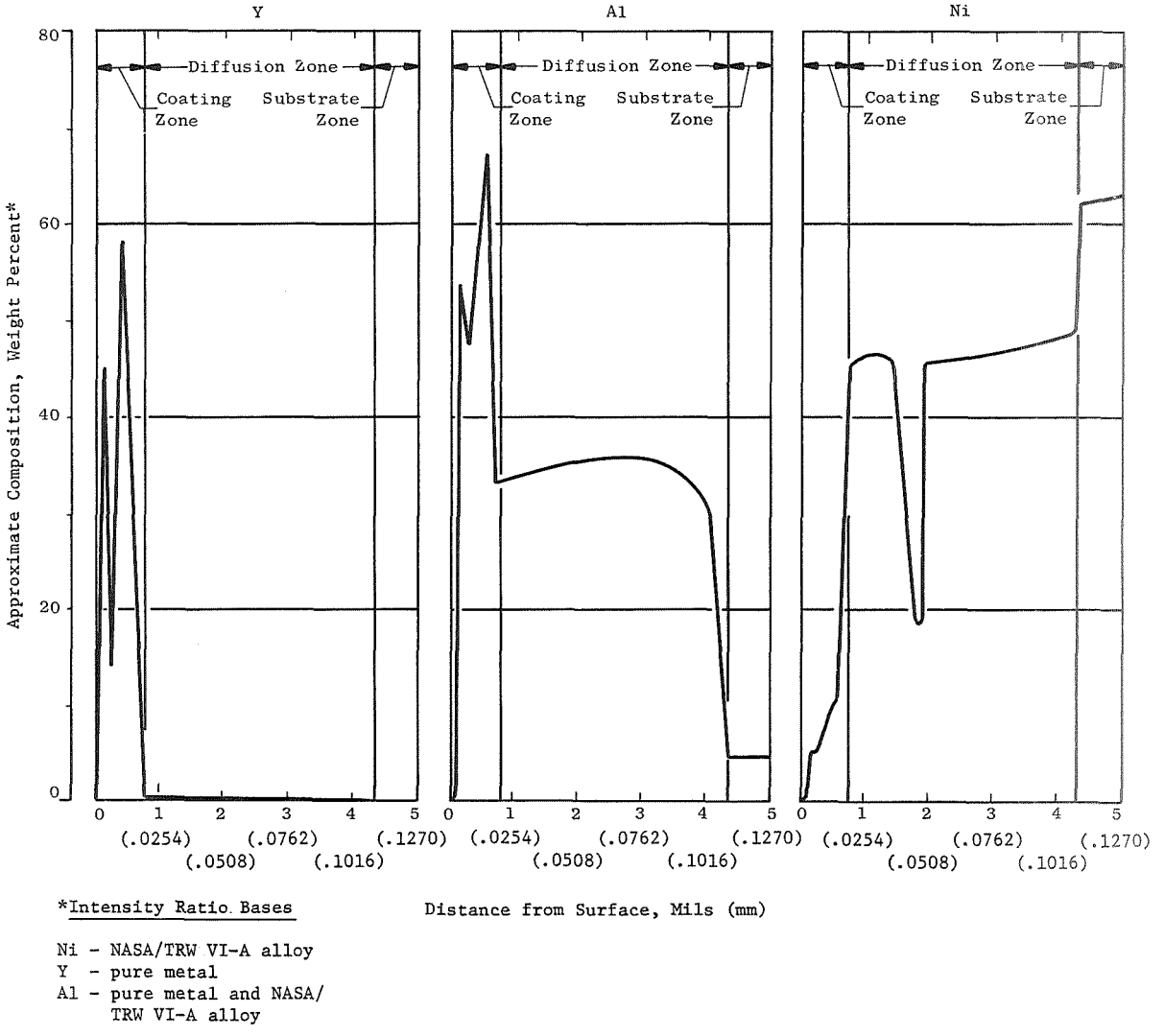

Figure 8. Microprobe Analysis of Al + Y Metallide System on NASA/TRW VI-A.

Poor adherence occurred between the Al and Ta layers, and only three of six development parameter sets were useable. Figure 9 shows a typical microstructure. Microprobe traces of the principal elements in this specimen are shown in Figure 10. The outer irregular light phase is shown to contain Al and Ta. The sublayer of irregular grey phase is high in Ta. The diffusion zone reveals gradients of Ni, Ta, and Al to base-metal composition levels. The selected parameters for Ta + Al metalliding are as follows:

Table IV. Selected Parameters for Tantaliding/Aluminiding.

Process Step	Operation	Temperature, °F (°K)	Current Density, ma/cm^2	Time, Hrs	Bath Composition*
1	Tantalide	1860 (1300)	5	16	0.3 TaF_5
2	Aluminide	1800 (1258)	6	8	0.3 AlF_3
3	Vacuum Treat	2200 (1478)	---	1	---
*Mol % in LiF					

3.1.7 Zr + Y, System 5

The order of metalliding these elements was reversed from the original plan, as in the other Y-containing systems, so that the lesser-activity element was applied first. Zirconiding was successful only when gettering techniques were used, as described in Section 3.1.4. Table V contains the parameters developed.

Attempts to apply Y resulted in eutectic melting of the Ni-Zr-Y system. Low current densities were tried, without success, in limiting the Y concentration. Samples came out of the bath with wrinkled surface appearance indicating that melting could not be avoided. Thus, this system was discontinued.

Table V. Metalliding Parameters for Development Specimens for the Zirconide System.

Sample No.	Temperature, °F (°K)	Current Density, ma/cm^2	Time, Hrs	Wt. Gain, mg/cm^2	Bath Composition*
106-6	1900 (1310)	1.2	7.5	9.5	0.3 ZrF_4
108-7	1750 (1232)	1.2	7.5	12.9	0.3 ZrF_4
110-1	1750 (1232)	0.6	16	15.8	0.3 ZrF_4
110-2	1750 (1232)	1.2	7.5	11.5	0.3 ZrF_4
110-3	1750 (1232)	0.6	16	17.5	0.3 ZrF_4
112-1	1900 (1310)	1.2	7.5	16.1	0.3 ZrF_4
*Mol % in LiF					

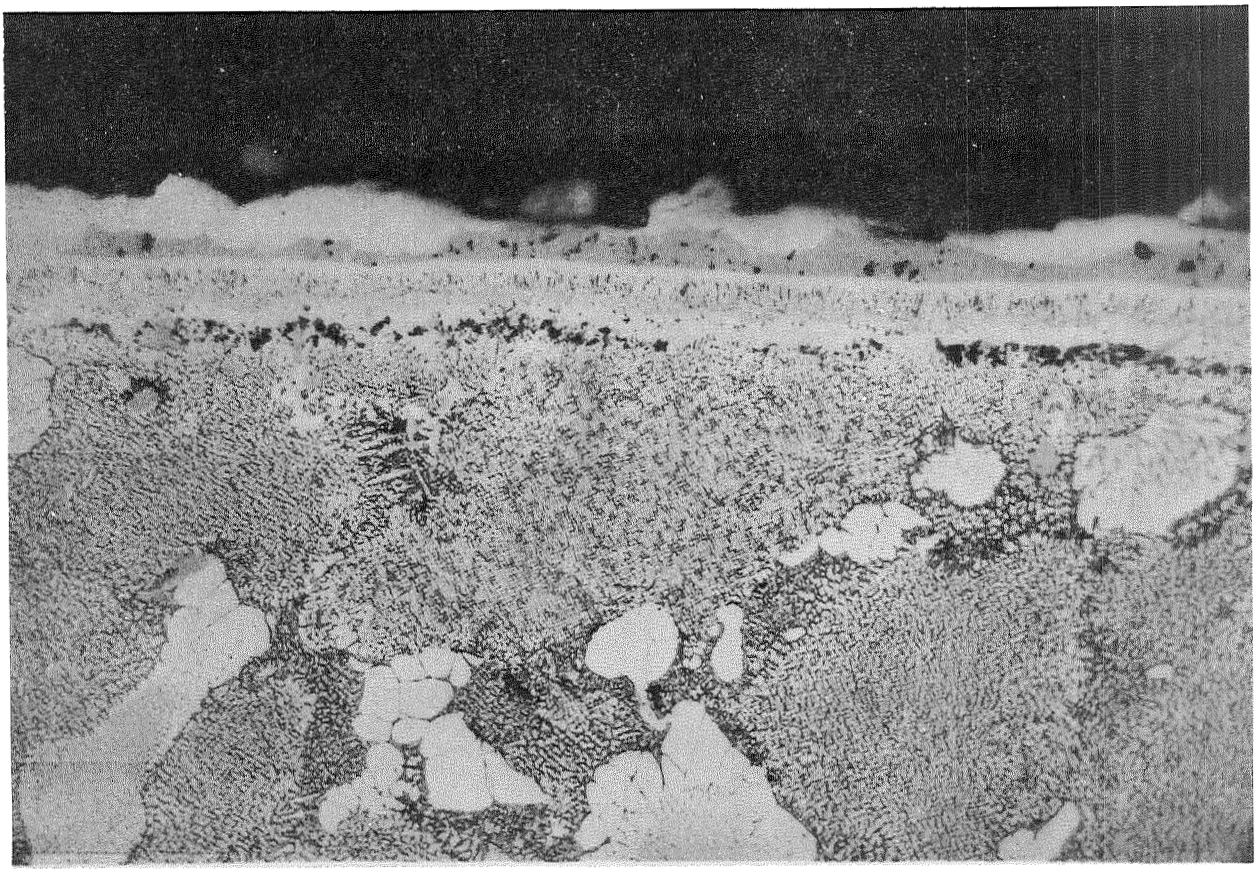

Figure 9. Tantalide/Aluminide System on NASA/TRW VI-A (Neg. B 11121, 500X, TRW Etch)

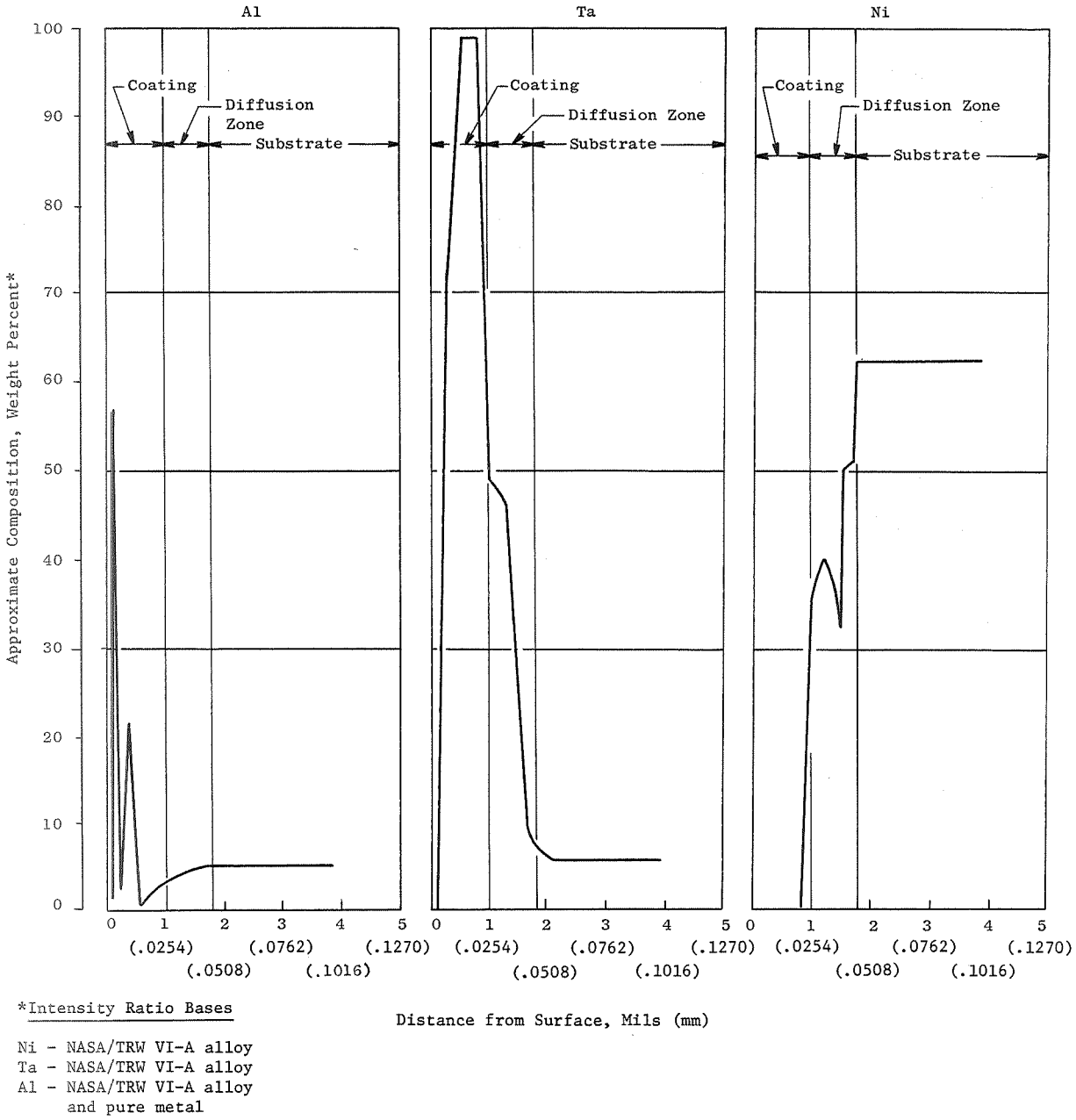

Figure 10. Microprobe Trace of Ta + Al Metallide System on NASA/TRW VI-A.

3.1.8 Al, System 6

Aluminiding as a single-element metalliding system was added to the program as a substitute for the unsuccessful Zr + Y and Y + Cr systems. This system was intended to provide a Ni-Al system obtained by metalliding the Al for comparison with General Electric's CODEP pack-process Ni-Al coating on IN-100.

System 6 parameters were the same as described for primary aluminiding in System 3.

3.2 METALLIDING OF TEST SPECIMENS

3.2.1 Mn + Cr

A summary of metalliding weight gain data for the preparation of System 1 oxidation test specimens is contained in Table VI. All but two specimens were processed through the postcoating heat treatment of 1 hour at 2200°F (1478°K) in vacuum.

Contamination of the chromiding bath by dissolution of Mn resulted in decreasing chromiding efficiency with each successive specimen. To alleviate the chromide bath contamination, the Mn was removed after each chromide run by plating out the dissolved Mn on a Cu screen, beginning with Panel Specimen 126-2 and Paddle Specimen 130-2. Weight gains for Cr applications were based on the original manganided weight. Since Mn is continually lost during chromiding, the Cr weight gain is in reality higher than it appears to be. Microprobe analysis confirmed the loss of Mn. Where the specimens contained about 40% Mn in the additive layer before chromiding, the Mn was depleted to only 1 to 10% after chromiding. This was previously shown in Figure 3. Loss of Mn would be expected during the longtime chromiding, which required low current densities and low-driving force. Bath contamination, of course, aggravated the condition.

3.2.2 Al + Y

A summary of metalliding weight gains for the preparation of Al + Y oxidation test specimens is contained in Table VII. Aluminiding was very consistent for all twelve specimens processed; however, yttriding of the initial specimens of each type (prefixes 103 and 125) was unsuccessful due to oxygen contamination from impure argon cover gas. A gettering system corrected the situation, and prefixed 174, 175, and 180 panels and paddles were prepared for oxidation tests.

3.2.3 Ta + Al

A summary of the metalliding weight gains for Ta + Al oxidation test specimens is contained in Table VIII. The processing was generally consistent and was only hampered by corrosion failure of the tantaliding cell during initial runs. Specimens prefixed 152 and 163 were prepared with a new cell.

Table VI. Metalliding Weight Gains of Manganide and Chromide Oxidation Test Specimens.

Description	Sample No.	Manganide			Chromide		
		Time, Hours	Temp., °F (°K)	Apparent Wt. Gain, mg/cm^2	Time, Hours	Temp., °F (°K)	Apparent Wt. Gain, mg/cm^2
Type A Coupons	104-5	5	1800 (1258)	11.8	24	1900 (1310)	14.5
	104-6	5	1800 (1258)	13.4	24	1900 (1310)	10.7
	107-3	5	1800 (1258)	11.9	24	1900 (1310)	6.7
	126-2	5	1800 (1258)	9.8	---	---	---
	126-4	5	1800 (1258)	9.9	24	1900 (1310)	8.5
	126-6	5	1800 (1258)	9.9	24	1900 (1310)	9.8
	130-1	5	1800 (1258)	10.5	24	1900 (1310)	11.5
Type B Paddle Wheel Specimens	111-2	5	1800 (1258)	11.4	24	1900 (1310)	1.1
	111-3	5	1800 (1258)	10.9	24	1900 (1310)	9.2
	126-3	5	1800 (1258)	11.4	24	1900 (1310)	---
	130-2	5	1800 (1258)	10.6	24	1900 (1310)	18.1
	130-3	5	1800 (1258)	10.8	24	1900 (1310)	10.1
	193-2	---	---	11.4	---	---	19.5
	193-4	---	---	11.8	---	---	10.2

Table VII. Metalliding Weight Gains of Aluminide and Yttride Oxidation Test Specimens.

Specimen	Sample No.	Aluminide			Yttride		
		Time, Hours	Temp., °F (°K)	Apparent Wt. Gain, mg/cm^2	Time, Hours	Temp., °F (°K)	Apparent Wt. Gain, mg/cm^2
Type A Coupons	103-3	8	1800 (1258)	14.2	---	---	---
	103-4	8	1800 (1258)	14.8	---	---	---
	103-5	8	1800 (1258)	15.1	---	---	---
	103-6	8	1800 (1258)	15.4	---	---	---
	175-2	8	1800 (1258)	13.9	2	1750 (1232)	1.9
	175-4	8	1800 (1258)	13.9	2	1750 (1232)	1.8
	175-6	8	1800 (1258)	15.2	2	1750 (1232)	1.0
	180-2	8	1800 (1258)	15.1	2	1750 (1232)	1.2
Type B Paddle Wheel Specimens	125-1	8	1800 (1258)	18.3	---	---	---
	125-2	8	1800 (1258)	18.2	---	---	---
	174-4	8	1800 (1258)	16.2	2	1750 (1232)	2.1
	174-6	8	1800 (1258)	16.7	2	1750 (1232)	1.6

Table VIII. Metalliding Weight Gains of Tantalide and Aluminide Oxidation Test Specimens.

Description	Sample No.	Tantalided			Aluminided		
		Time, Hrs	Temp., °F(°K)	Apparent Wt. Gain, mg/cm^2	Time, Hrs	Temp., °F(°K)	Apparent Wt. Gain, mg/cm^2
Type A Coupons	119-4	16	1850 (1289)	36.9	8	1800 (1258)	17.9
	119-5	16	1850 (1289)	30.8	8	1800 (1258)	15.9
	152-3	16	1850 (1289)	31.1	8	1800 (1258)	11.8
	163-3	16	1850 (1289)	22.8	8	1800 (1258)	12.9
Type B Paddle Wheel Specimens	122-4	16	1850 (1289)	30.1	8	1800 (1258)	20.0
	122-6	16	1850 (1289)	26.5	8	1800 (1258)	14.9

3.2.4 Al

Weight gain data for this single-element metalliding, substituted for the unsuccessful Zr + Y system, are contained in Table IX. Aluminiding was consistent and without processing problems. Four specimens prefixed 136 were evaluated in static oxidation.

3.3 BALLISTIC IMPACT TESTING

Adherence of the metallided coatings was evaluated by ballistic impact using a modified air rifle propelling an alloy steel ball 0.175 inch (4.445 mm) in diameter and weighing 0.355 gm, at a velocity of 500 ft/sec (152 m/sec). The ball velocity was monitored by photoelectric timers. Charging of the gun was by bottled compressed nitrogen. Specimens were tested at room temperature and were induction heated for impacting at 1900°F (1310°K).

The Mn + Cr specimens were the only ones that did not exhibit damage after either room temperature or elevated temperature impacting. All the other coated specimens were cracked and spalled on the crater side from the room temperature impacting. No system exhibited visible macroscopic tensile-side damage until during the oxidation tests. The Al + Y specimen then developed severe tensile-side oxidation, and metallography revealed cracks in the other systems.

Testing at elevated temperature improved the impact resistance of all systems. No cracking or spalling was visible on a macroscopic basis. Increased ductility was evidenced by the larger crater diameters occurring in each heated specimen. There was no significant influence of the coatings, since all specimens (including the uncoated ones) exhibited craters of generally equal diameter, except as influenced by temperature.

3.4 STATIC OXIDATION TESTING

3.4.1 Thermal Cycle Schedule

Table X itemizes the specimen preparation and final weight change results for the static oxidation specimens. The static oxidation specimens were subjected to the following thermal cycle and weighing schedule:

1. One thermal cycle to 2000°F (1367°K), holding two hours at temperature, then a 5-minute quench to room temperature for weighing. This was repeated twelve times to accumulate the first 24 hours of time at temperature and weight change data, followed by:

2. Three thermal cycles to 2000°F (1367°K), holding two hours at temperature with intermediate 5-minute quenching to room temperature; then, a final hold of 16 hours at 2000°F (1367°K) and a 5-minute quench to room temperature for weighing. This pattern was repeated 8 times to accumulate the remaining 176 hours of time at temperature and weight change data.

Table IX. Metalliding Weight Gains of Aluminided Oxidation Test Specimens.

Description	Sample No.	Time, Hours	Temp, °F(°K)	Weight Gain, mg/cm^2
Type A Coupons	136-1	8	1800 (1258)	19.6
	136-2	8	1800 (1258)	17.3
	136-3	8	1800 (1258)	17.0
	136-5	8	1800 (1258)	17.3
Type A Coupons	180-4	8	1800 (1258)	14.9
	180-5	8	1800 (1258)	14.8
	184-1	8	1800 (1258)	15.2
	136-2	8	1800 (1258)	16.5

Table X. 2000°F (1367°K) Static Oxidation Test Results.

System	Metalliding Specimen Nos.	Prior Impact	Total Test Time, hrs.	Total Weight Change, mg/cm^2
1) Mn + Cr	130-1/150-5	None	156	- 21.9
	126-4/157-2	1900°F (1310°K)		- 24.9
	104-6/116-2	Room Temperature		- 26.7
	126-6/154-1	None		- 27.0
3) Ta + Al	119-5/125-6	None	156	- 26.7
	122-1/125-5	1900°F (1310°K)		- 15.7
	163-3/161-5	Room Temperature		- 8.6
	152-3/151-2	None		- 23.1
4) Al + Y	175-6/182-6	1900°F (1310°K)	200	- 2.3
	175-2/183-4	Room Temperature		- 2.7
	180-2/186-4	None		- 3.2
	175-4/186-2	None		- 2.6
6) Al	136-2	1900°F (1310°K)	200	- 0.4
	180-5	Room Temperature		+ 0.1
	180-4	None		- 0.2
	184-1	None		- 0.4

During the 200 hours of exposure, each specimen was subjected to a maximum of 44 thermal cycles, and 20 weighings. Weight change data characteristically indicated the initial weight gains from adherent oxides, followed by losses due to spalling. The weight change data are plotted in Figure 11, as averages for the specimens as listed in Table X.

3.4.2 Mn + Cr

Coating System 1 oxidized and spalled rapidly. Specimens exhibited weight losses after the second thermal cycle and continued a sharp decline throughout the remaining exposure. Testing was continued for 158 hours to determine whether a resistant phase might develop and stabilize the system. None was evident when the test was terminated.

Figure 12 illustrates the surface appearance of the specimen with spalling clearly visible. Figure 13 shows a metallographic section of the impact areas of the 1900°F (1310°K) specimen. Loss of coating is evident not only as a spalled patch on the impact side, but also loss of coating is complete on the opposite surface. Furthermore, intergranular oxidation is evident.

Figure 14 is a photomicrograph showing an area of the specimen with the primary diffusion layer separated from the substrate. The appearance reflects the gross weight loss indicative of spalling which was shown in Figure 12. The coating spalled along the original boundary of the metallided diffusion zone. This boundary appeared as a dark band in the as-coated structure shown in Figure 4.

Figure 15 shows the electron microprobe back scatter (EBS) and individual scans of the metallided and principal base-metal elements. They show a very low residual concentration of Mn in the spalled layer; the very high concentration of Cr indicates the oxide layer and inclusions to be mainly chromium oxide. Microprobe traces of the Mn and Cr confirm less than 1% Mn and a peak of 50% Cr, as illustrated in Figure 16.

The principal elements of the NASA/TRW VI-A alloy are generally shown to be uniformly present in the spalled layer at about the same intensity as in the substrate, except for the area of high Cr content. The trace of Ni shows the expected substrate concentration of 62% and indicates Ni-lean areas in the surface coating layer. A Ta-rich phase is shown in the spalled layer, possibly $TaCr_2$. The presence of TiC is also a possibility indicated by Ti-rich phases in the diffusion zone.

Al is shown in high concentration at the spall line and as spotty inclusions within the substrate. This is attributable to oxidation effects on the exposed substrate after the outer coating layer spalled.

3.4.3 Al + Y

Coating System 3 was generally protective, largely due to the aluminided coating layer. After an initial gain, there was little change for the first

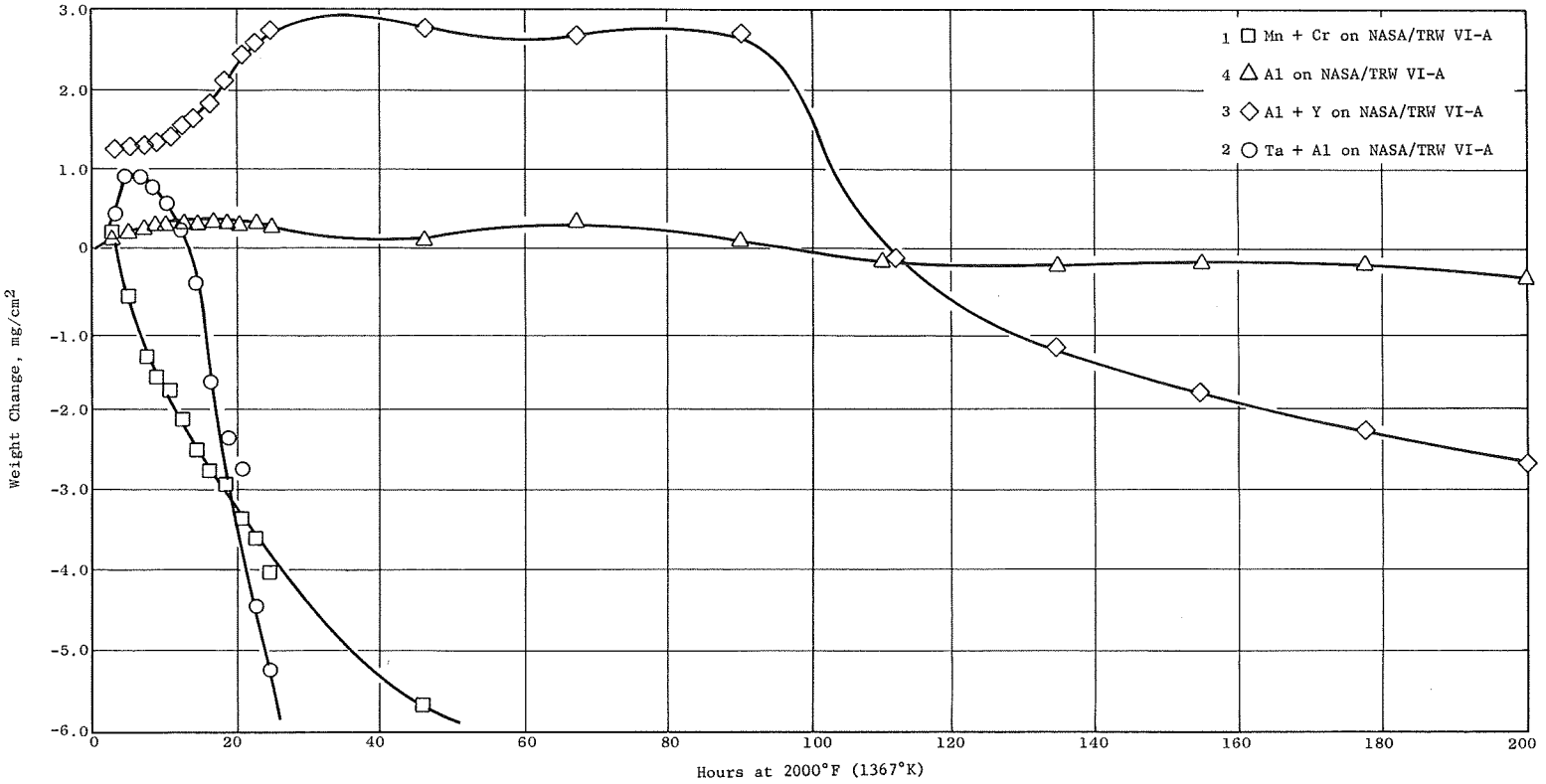

Figure 11. Static Air Furnace Oxidation Test Results for Sequentially-Metallided Dual-Element Coating Systems on NASA/TRW VI-A. As Shown by Data Points, Specimens Were Thermal Cycled and Weighed Every 2 Hours During First 24 Hours, Then in Patterns of Three 2-Hour Holds Plus One 16-Hour Hold During the Test Duration.

Figure 12. Appearance of Manganide/Chromide System After 158 Hours Static Oxidation at 2000°F (1367°K) (C70052709, 10X).

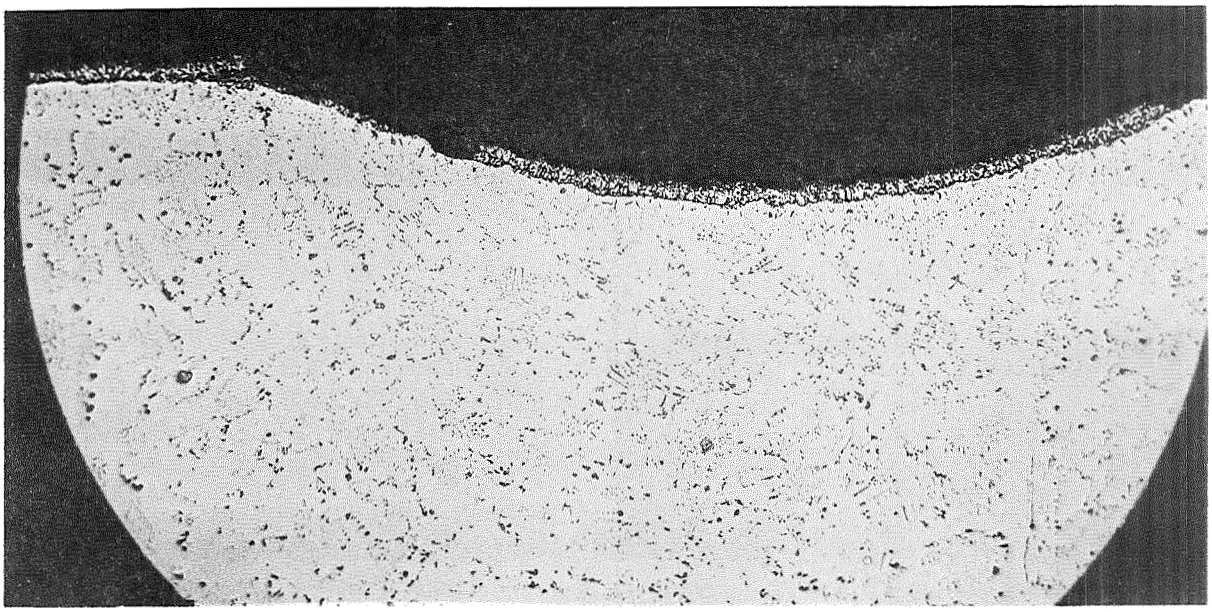

A. Impacted Surface

B. Surface Opposite Impact

Figure 13. 1900°F (1310°K) Ballistic Impact Site on Mn + Cr Metallide System After 200 Hours Static Oxidation at 2000°F (1367°K). Intergranular Oxidation May be Seen on the Surface Opposite Impact (F 6007, F 6008, 50X).

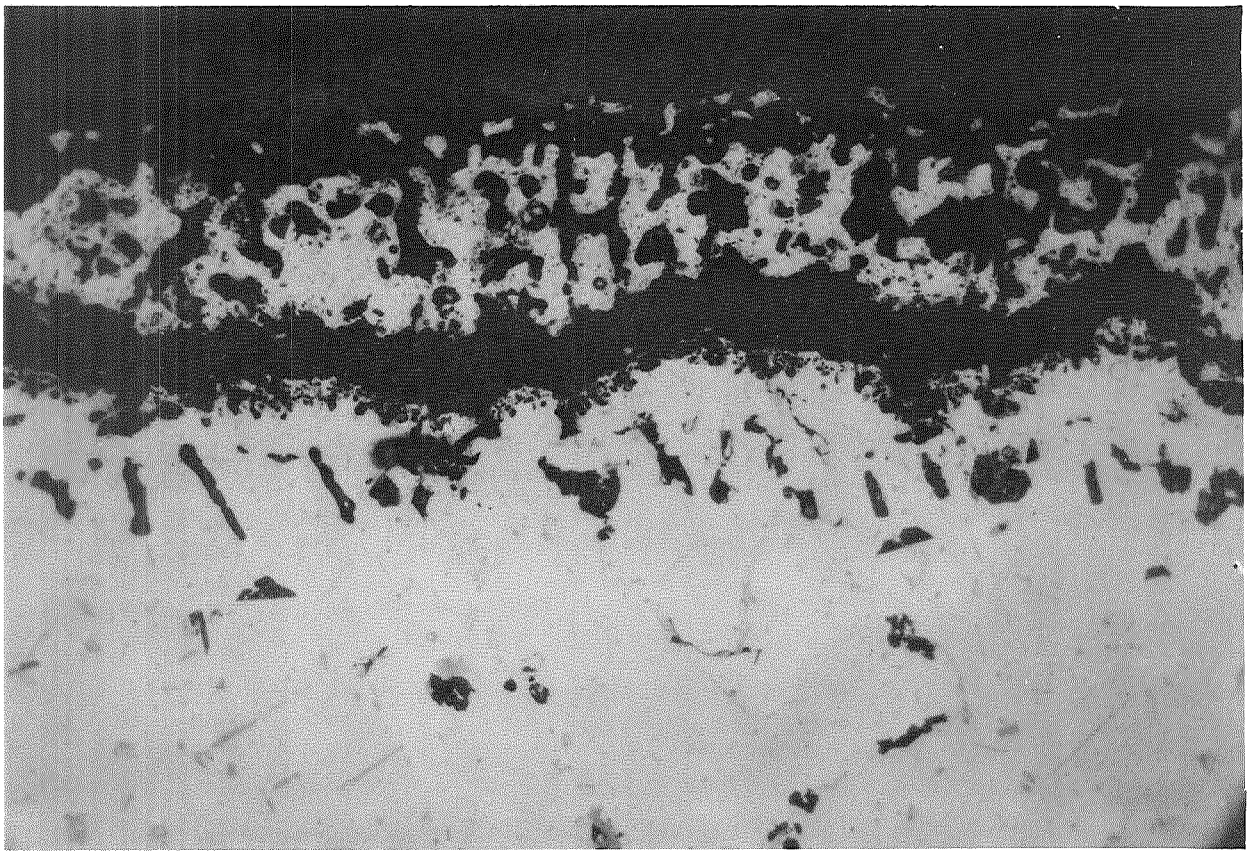

Figure 14. Mn + Cr Metallide System After 152 Hours Static Oxidation at 2000°F (1367°K) (F 6003, 500X, Unetched).

Metallided Elements Mn + Cr and Ni Base

Substrate Elements

Substrate Elements

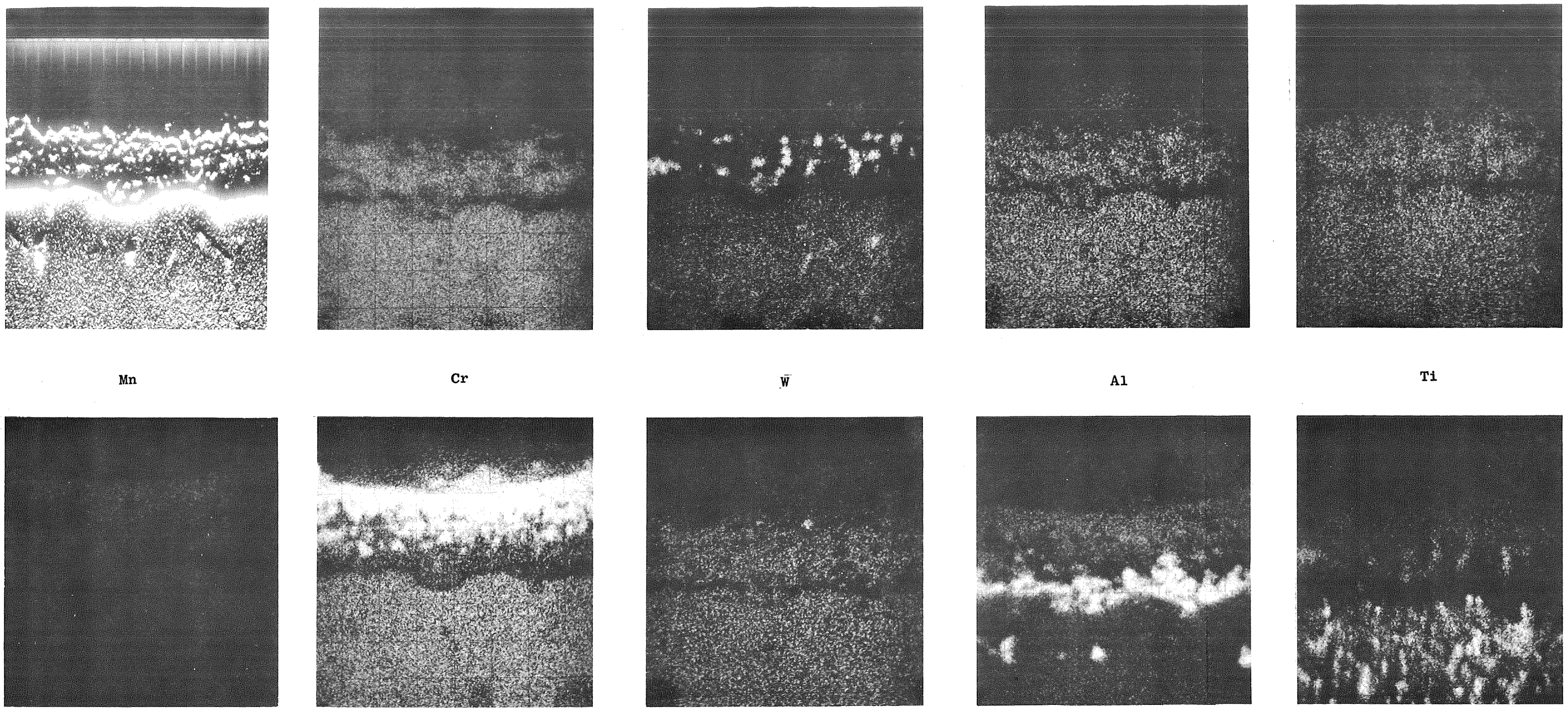

Figure 15. Microprobe Scans of Mn + Cr Metallide System on NASA/TRW VI-A After 152 Hours Static Oxidation at 2000°F (1367°K) (Mount E 4696, 360X).

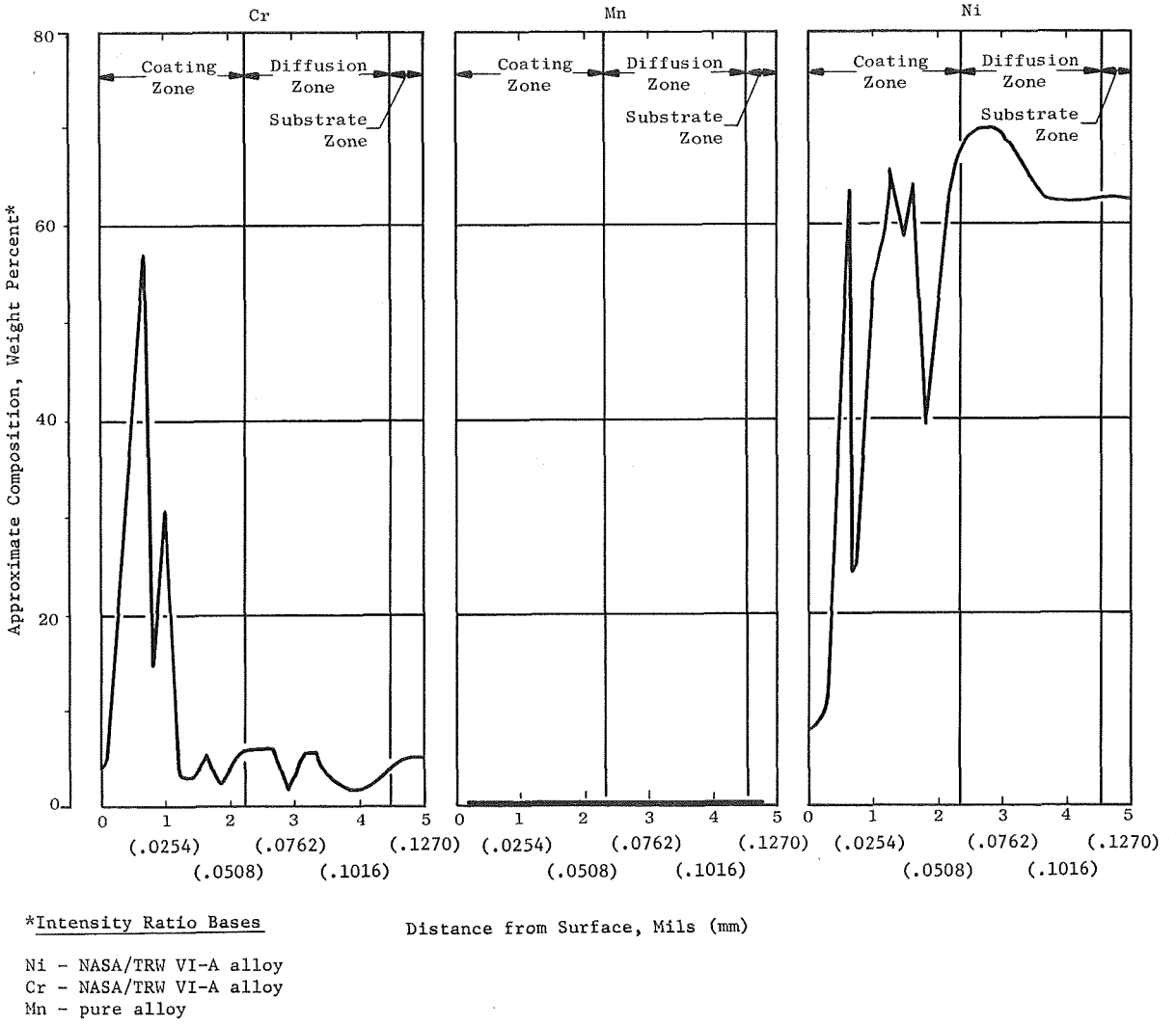

Figure 16. Microprobe Traces of Mn + Cr Metallide System on NASA/TRW VI-A After 158 Hours Static Oxidation at 2000°F (1367°K) (E 4696).

100 hours of testing, as shown by the weight change data in Figure 11. Then a very limited gradual weight loss occurred, along with a corresponding color change from gray to off-white. Figure 17 illustrates the general surface appearance. During the 200-hour exposure, the opposite surface of the ballistic impact impressions developed sites of severe oxidation. Gross spalling is evident; however, the adherence of the surrounding coating is apparent also. Figure 18 illustrates the microscopic appearance of the impact impression and opposite surface of the 1900°F (1310°K) impacted specimen. While not as severely affected as the room temperature impacted specimen, it also revealed spalling on the back side as exposure progressed. The coating layer is seen in Figure 18 to be 4 to 5 mils (0.1016 - 1.270 mm) thick, and the interdiffusion zone into the substrate is about 2-3 mils (0.0508 - 0.0762 mm) thick. The coating was dense and well bounded (unlike the Mn + Cr system) with no gross internal attack, except as previously noted for the impact sites, and a few cracks.

Initially, the Al-Y layer was visible as a light-colored material. This was consumed by oxidation in the first 100 hours. The remaining coating was mainly aluminide, and it oxidized gradually by surface attack. Figure 19 illustrates the appearance and shows the superficial oxide scale with no evidence of gross internal attack or stringer penetration. The coating, however, contained many fine but deep cracks such as is illustrated. Only a few were oxidized, indicating they originated internally and had not been exposed to the oxidizing environment. Propagation and initiation of such nonoxidized cracks may also have been the results of stresses induced or residual restraint relieved during cutoff and metallographic preparation. However, their presence indicates a situation potentially not desirable in a gas turbine engine.

Electron microprobe photographs, Figure 20, reveal the concentration of Al in the thin surface oxide layer and throughout the metallided zone and diffusion zone. Y was not detectable. Ni, Co, and Cr appear uniformly distributed throughout both zones except for areas void of Ni in the diffusion zone. Microprobe traces in Figure 21 confirm the distribution of Ni at 60-65% on either side of an area that has Ni minimums to 20-40%. Al is shown to be present in the primary layer at 12%, decreasing to 5-6% in the substrate. Y was not detected.

The Ni depletion is attributable to the presence of Ta-, W-, and Ti-rich phases in the diffusion zone, probably solid solutions of Ta-W and Ta-Ti. These are apparent in the electron photographs. The Ta-rich phase distribution is particularly evident in the diffusion zone, but is also present in the primary diffusion layer and as a thin surface layer.

3.4.4 Ta + Al

System 4 specimens failed rapidly due to spalling within 20 hours of exposure as indicated by the weight loss data in Figure 11. Figure 22 illustrates the typical surface appearance with spalling evident. Figure 23 illustrates spalling and coating deterioration at the impact sites. Figure 24 is the typical metallographic appearance showing spalling and oxide penetration.

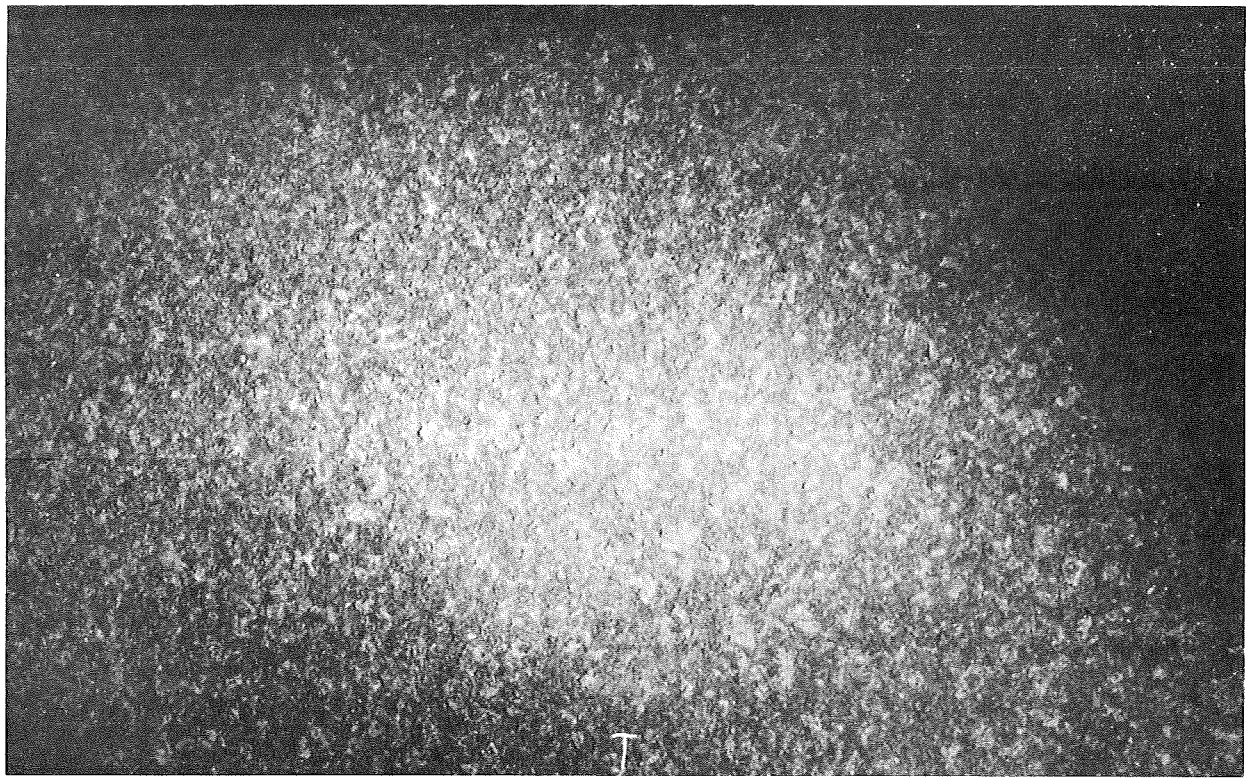

Figure 17. Surface Appearance of the Aluminide/Yttride System After 200 Hours Static Oxidation at 2000°F (1367°K) (C70052714, 10X).

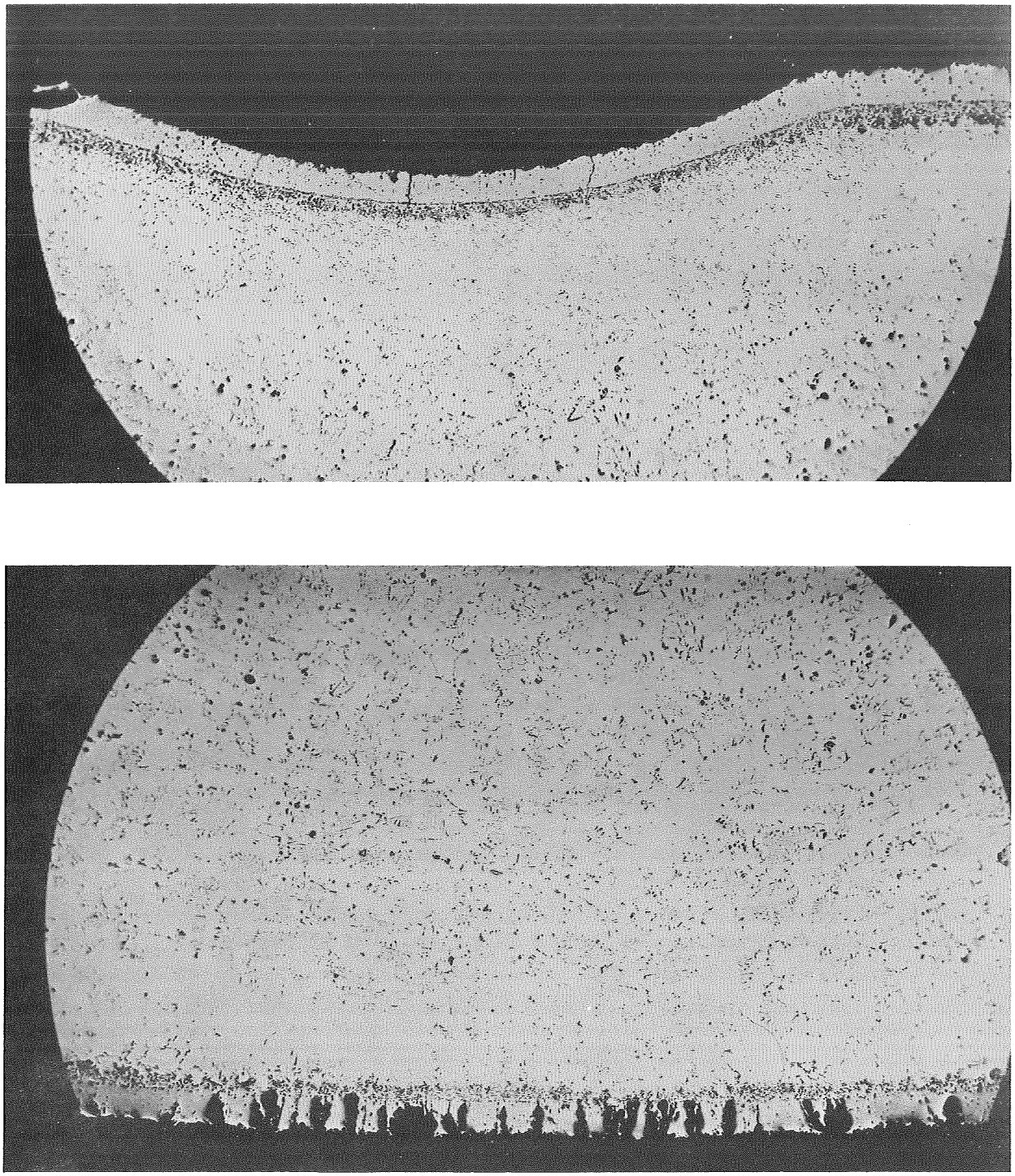

Figure 18. Ballistic Impact Sites 1900°F (1310°K) Impact on Al + Y Metallide System After 200 Hours Static Oxidation at 2000°F (1367°K) (F 6009, F 6010, 50X).

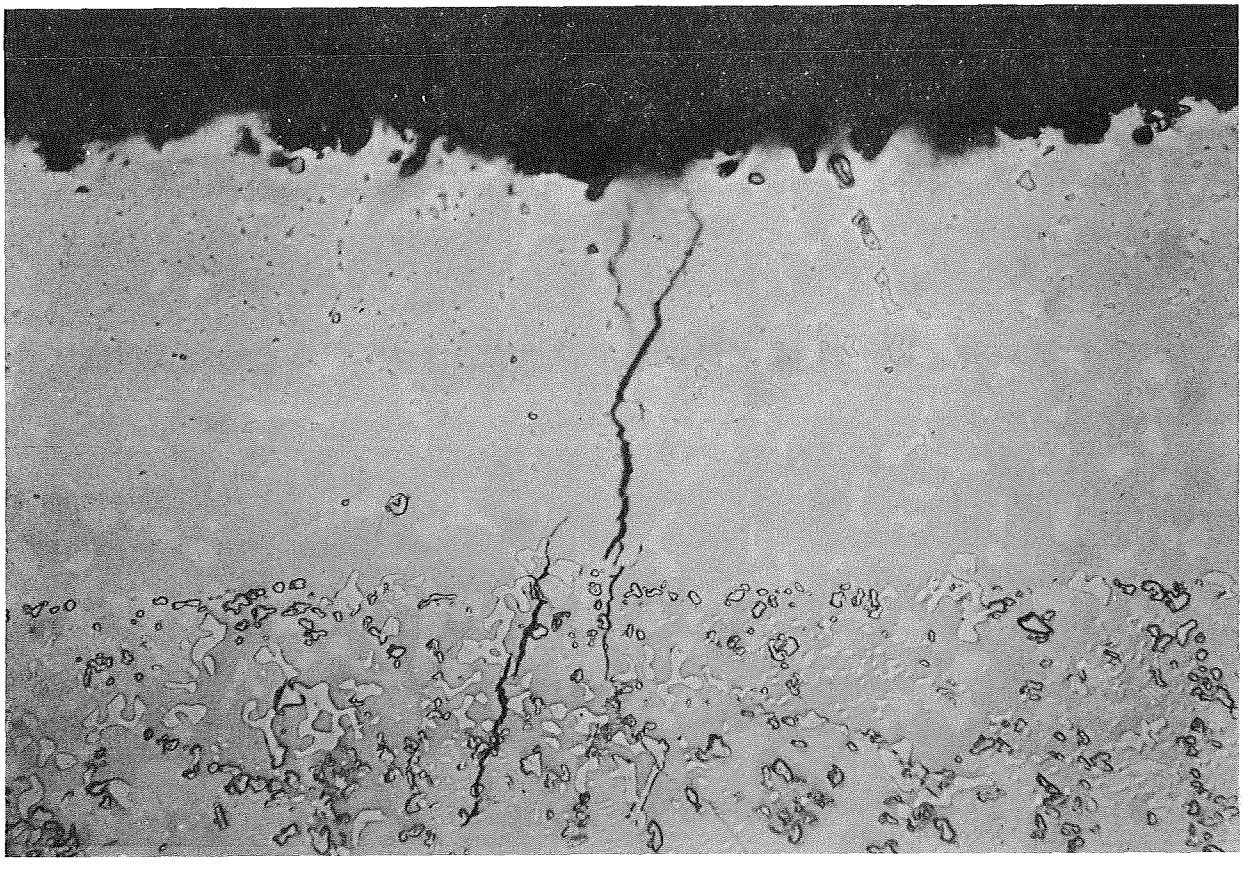

Figure 19. Al + Y Metallided System on NASA/TRW VI-A After 200 Hours Static Oxidation at 2000°F (1367°K) (F 6005, 500X, Unetched).

Metallided Elements Al + Y and Ni Base

Substrate Elements

Substrate Elements

EBS

Ni

Ta

Co

Mo

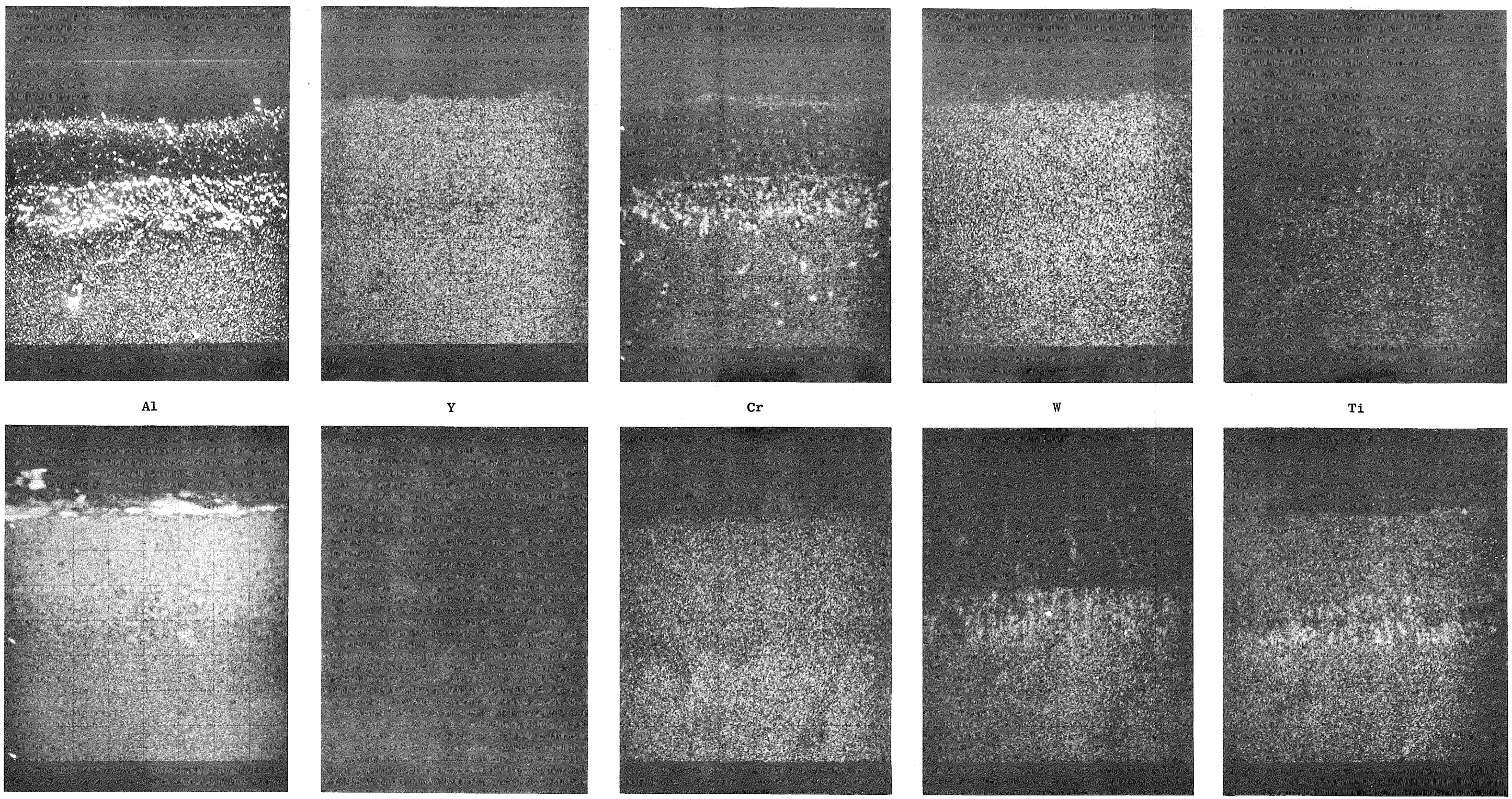

Al

Y

Cr

W

Ti

Figure 20. Microprobe Scans of Al + Y Metallide System on NASA/TRW VI-A Showing Metallided Elements and Ni Base After 200 Hours Static Oxidation at 2000°F (1367°K) (Mount E 4700, 360X).

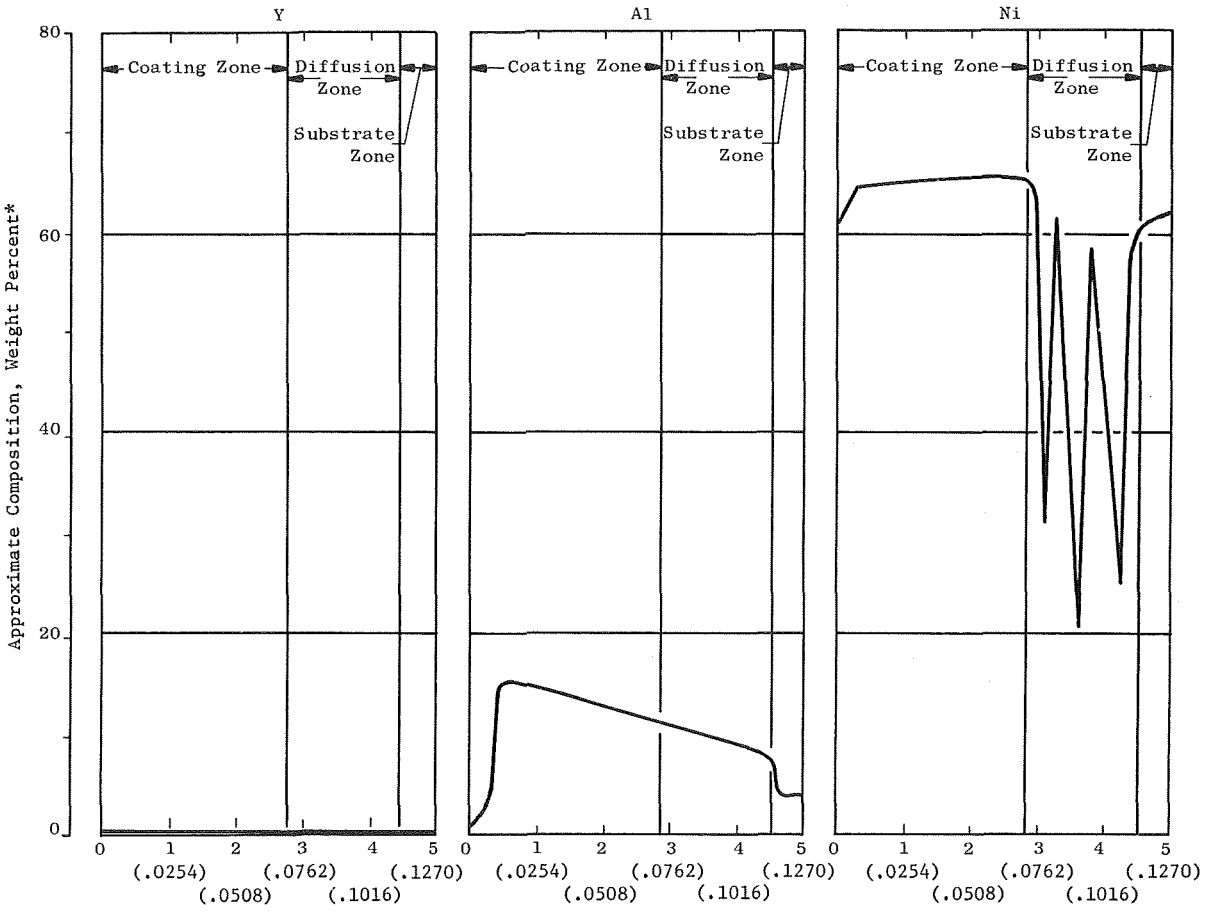

*Intensity Ratio Bases

Ni - NASA/TRW VI-A alloy
Y - pure metal
Al - pure metal and NASA/ TRW VI-A alloy

Figure 21. Microprobe Traces of Al + Y Metallide System After 200 Hours Static Oxidation at 2000°F (1367°K) (E 4700).

Figure 22. Natural Surface Spalling of the Tantalide/Aluminide System After 200 Hours Static Oxidation at 2000°F (1367°K) (C70052710, 10X).

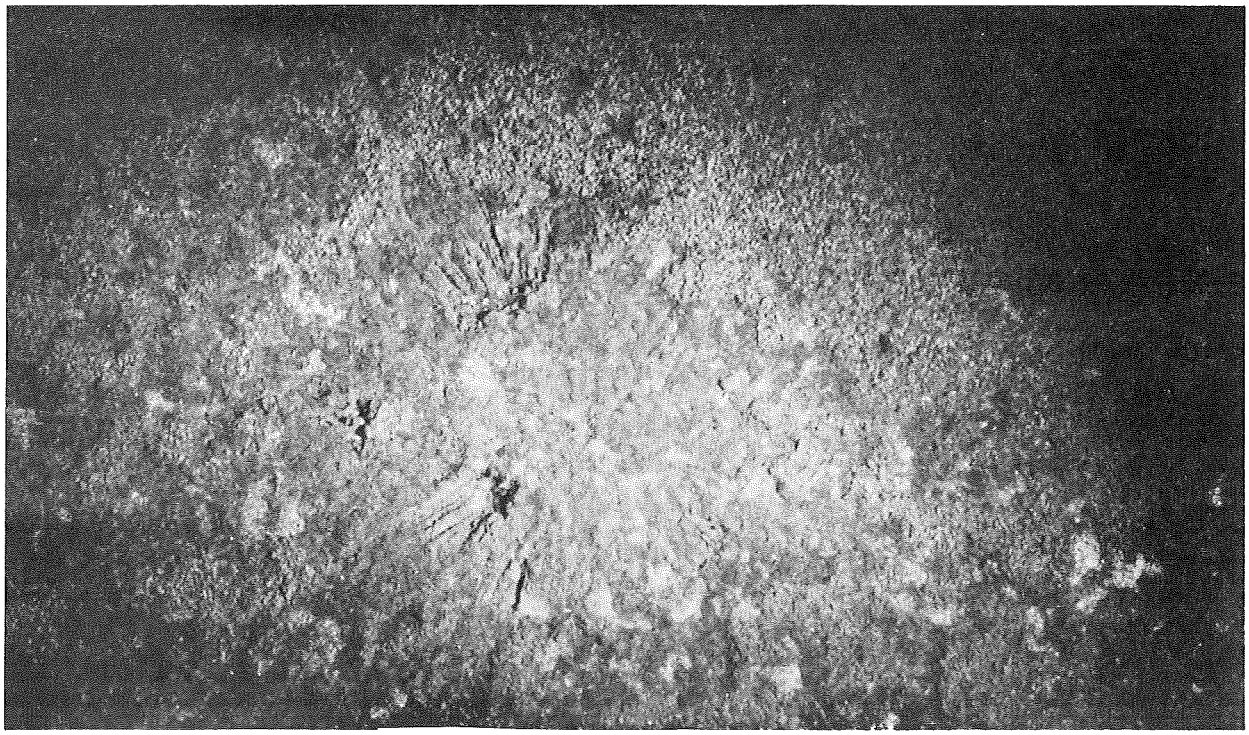

B. Surface Opposite Impact

Figure 23. Macroscopic Appearance of Ballistic Impact Sites on Ta + Al Metallided System After 200 Hours at 2000°F (1367°K) (C70052719, C70052720, 10X).

Figure 24. Microstructure of Ta + Al Metallide System on NASA/TRW VI-A After 200 Hours Static Oxidation at 2000°F (1367°K) (F 6004, 500X, Unetched).

The EBS photomicrographs in Figure 25 show residual amounts of the primary coating elements. This system differed in that there was no apparent interdiffusion layer. The oxide was Al_2O_3, and the primary diffusion zone contained Ta-rich phases. The primary zone also was enriched with W and contains Ti phases. The matching distribution of these solid solution phases was not evident. Mo-rich phases extend from the substrate into the outer layer. The distribution of Ni and the metallided elements in the EBS scans is confirmed by the microprobe traces shown in Figure 26. Ta peaks indicate very rich concentrations in the primary diffused coating layer, whereas the Al is essentially at substrate concentration levels of 5-7% except for surface enrichment to a peak of about 50%. Ni is lean at the surface, but its presence increased sharply to irregular concentrations between 40 and 62% and then leveled out at the substrate concentration of about 62%.

3.4.5 Al

The aluminided coating specimens were essentially similar in appearance to those of the Al + Y system. These specimens exhibited the only stable performance of the metallided systems tested in static oxidation. As was shown in Figure 11, they underwent a very small initial weight gain and virtually no further weight change throughout the 200-hour exposure. The surface appearance is shown in Figure 27.

Figure 28 is a typical microstructure of the aluminided coating after test, and the similarity to the Al + Y system may be observed by comparing previous Figure 19. The primary diffused outer layer was about 5 mils (0.1270 mm) thick, dense, and integral with the intermediate diffusion zone of the substrate. Although the coating also exhibited the same fine cracks all around the specimen perimeter, they showed no evidence of oxidation. It is concluded (as in System 3) that the cracks initiate internally and propagate when the metallographic specimen is cut. Close examination of the cracks reveals that they propagate through certain phase particles which appear with dark outlines, causing them to fracture in the crack path. The phase which is more globular and without an outline, probably Ni_3Al, appears to favor propagation around its boundary.

Figure 29 illustrates a ballistically-impacted specimen after oxidation. This specimen had been impacted at room temperature and as previously reported, was badly spalled and then oxidized at the impact site. The elevated-temperature impacted specimen was not badly spalled but suffered damage and subsequent oxidation on the impact surface.

Figure 30 shows the microprobe EBS and individual element scans of an aluminided specimen after the 200-hour static oxidation at 2000°F (1367°K). Again, the similarity to System 3 is evident. Deep secondary diffusion of Al is evident to nearly twice the coating layer thickness. The microprobe trace of Al in Figure 31 reveals a level of 16% Al in the primary coating layer and the presence of Ni_3Al. Also shown is a spiked interdiffusion zone and then a level substrate concentration of 5-6%. Ni is seen to be at 64-65% in the primary coating and about 61% in the substrate. The trace of the

Metallided Elements Ta + Al and Ni Base

Substrate Elements

Substrate Elements

EBS

Ni

Co

Mo

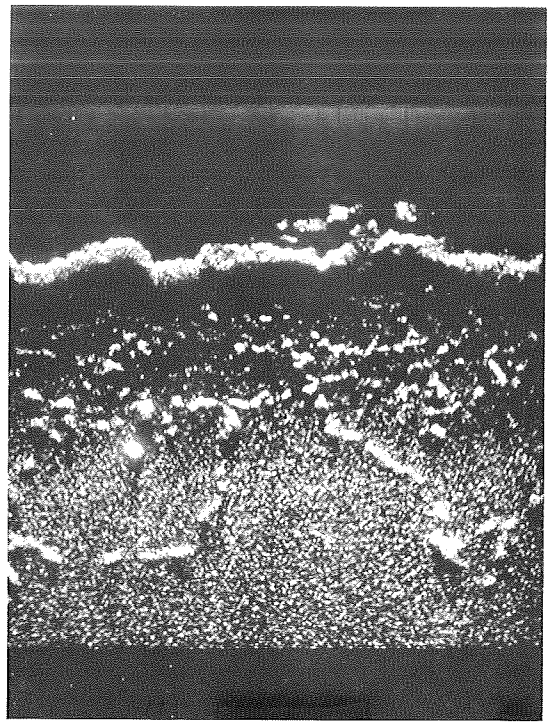

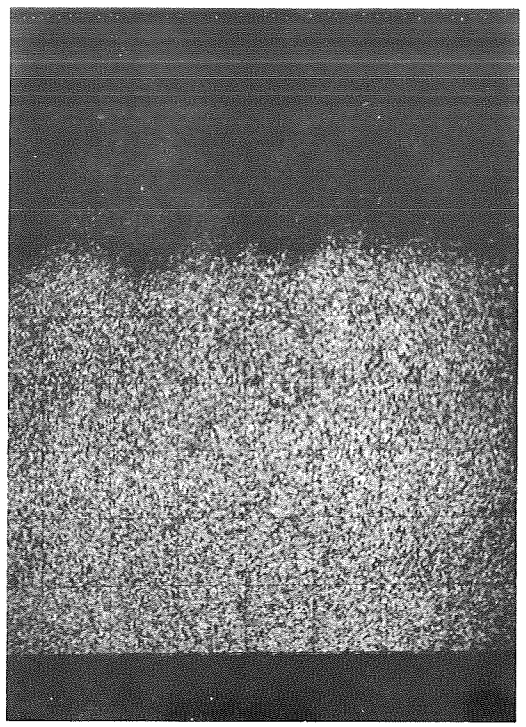

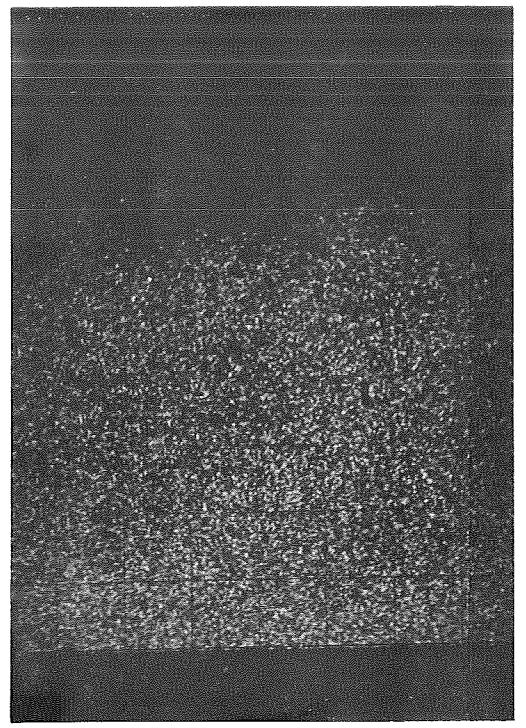

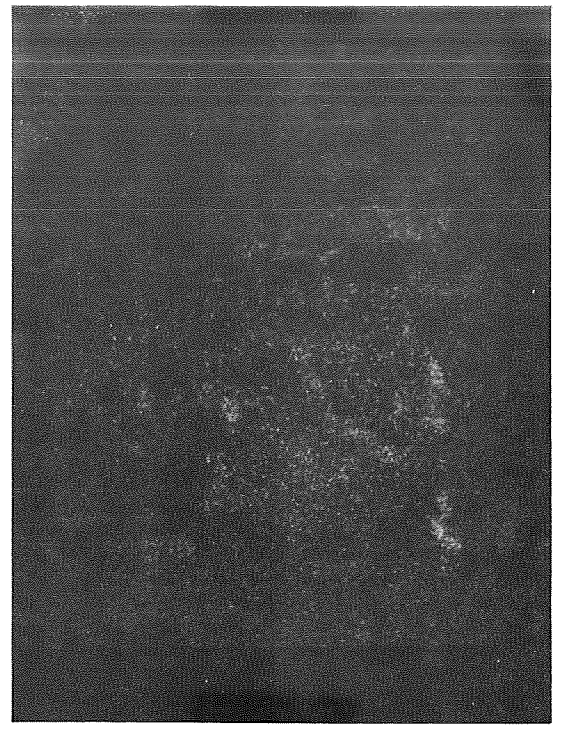

Ta

Al

Cr

W

Ti

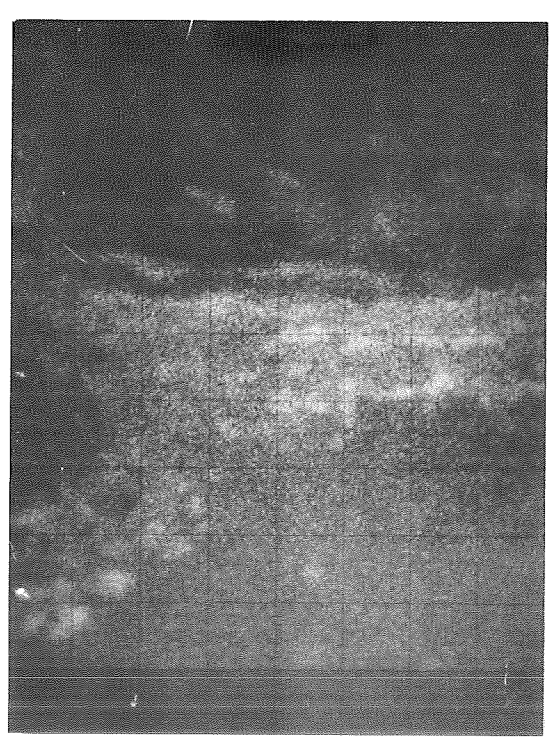

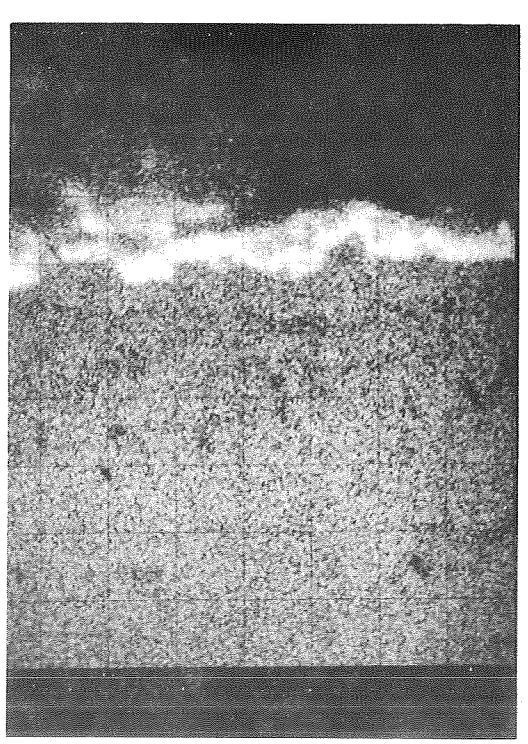

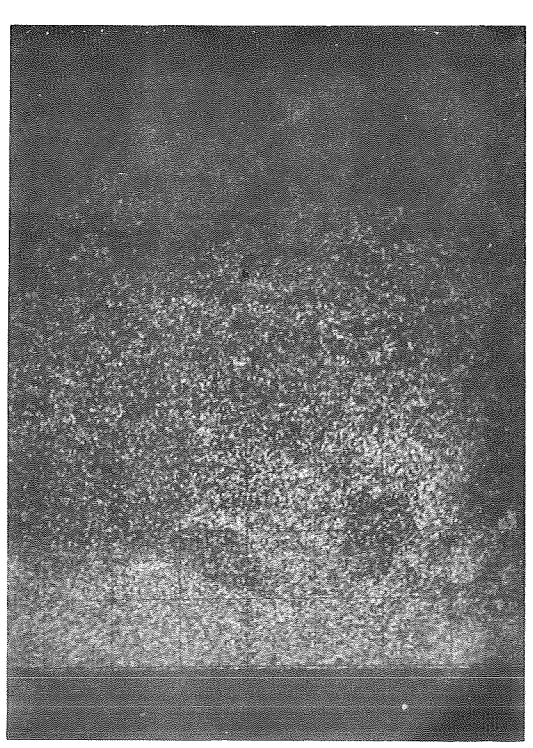

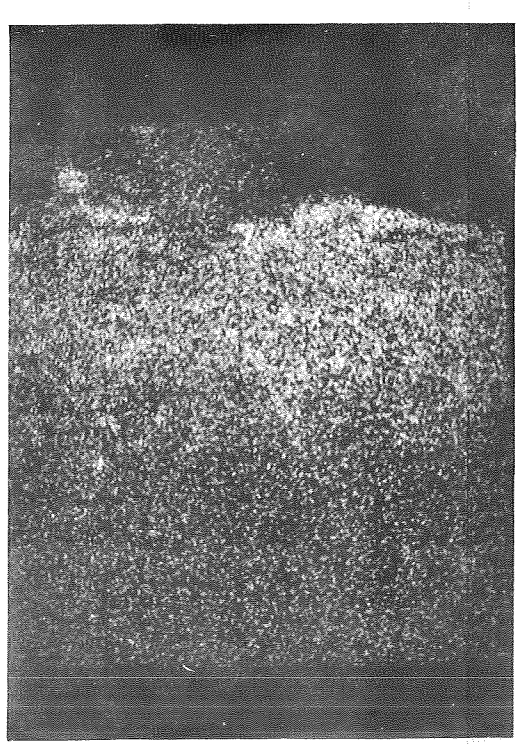

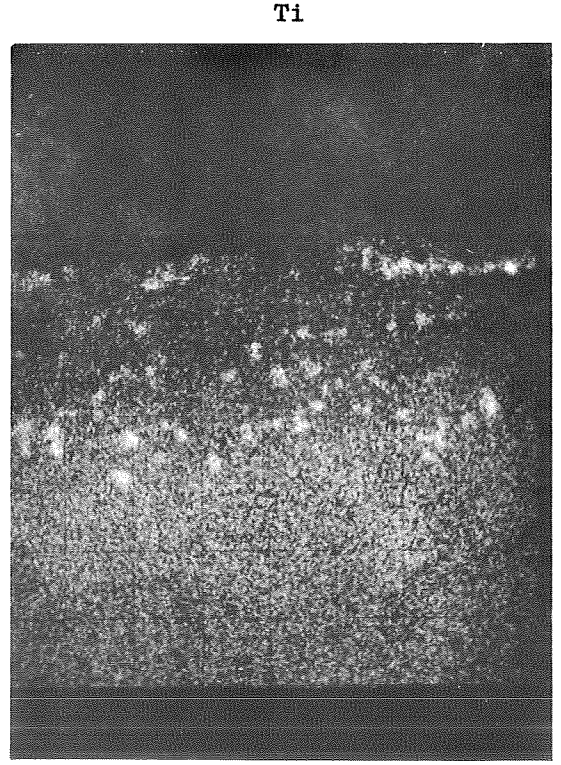

Figure 25. Microprobe Scans of Ta + Al Metallide System on NASA/TRW VI-A Showing Metallided Elements and Ni Base After 200 Hours Static Oxidation at 2000°F (1367°K) (E 4698, 360X).

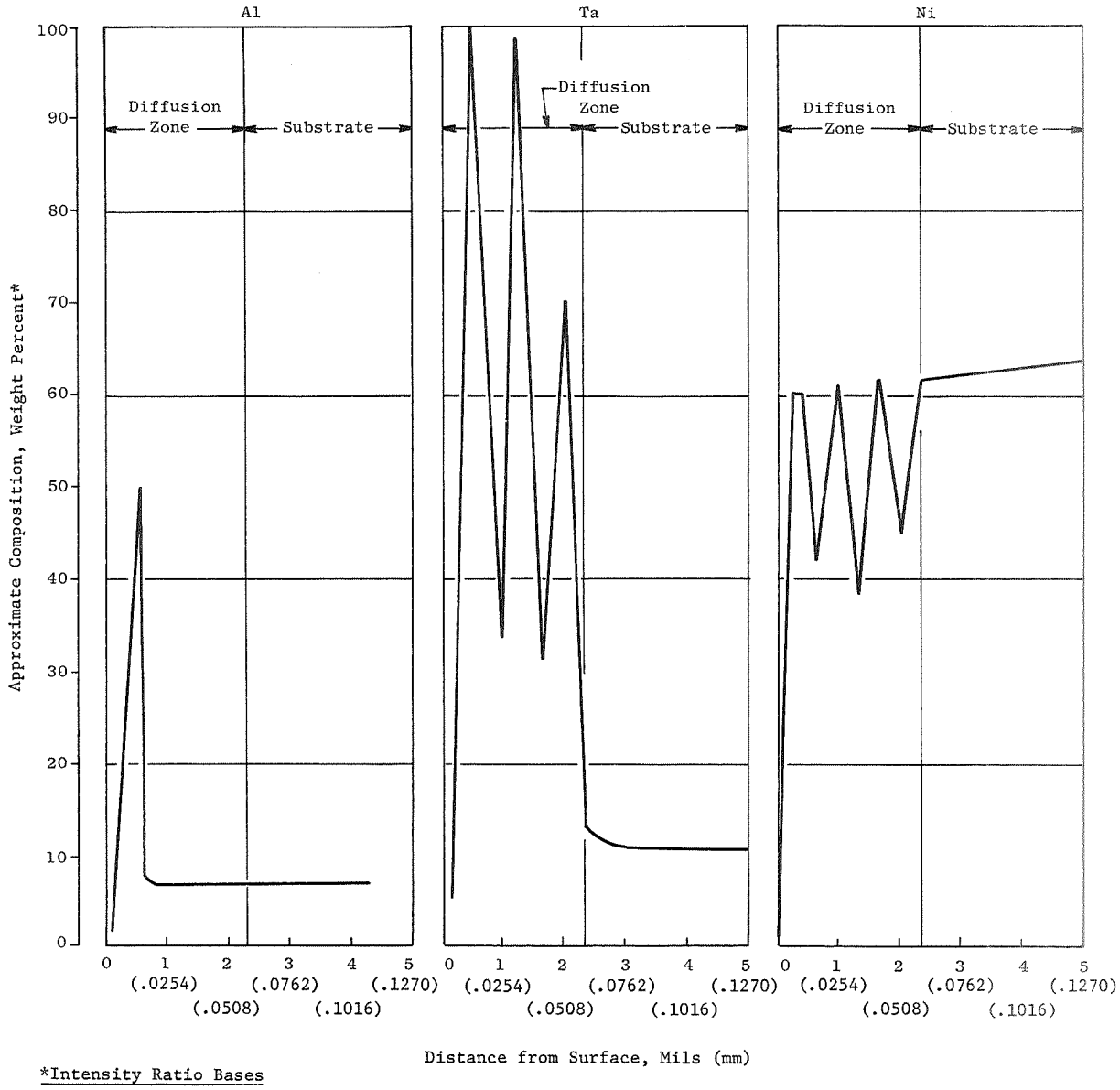

*Intensity Ratio Bases

Ni - NASA/TRW VI-A alloy
Ta - NASA/TRW VI-A alloy
Al - NASA/TRW VI-A alloy and pure metal

Figure 26. Microprobe Traces of Ta + Al Metallide System After 200 Hours Static Oxidation at 2000°F (1367°K) (E4689).

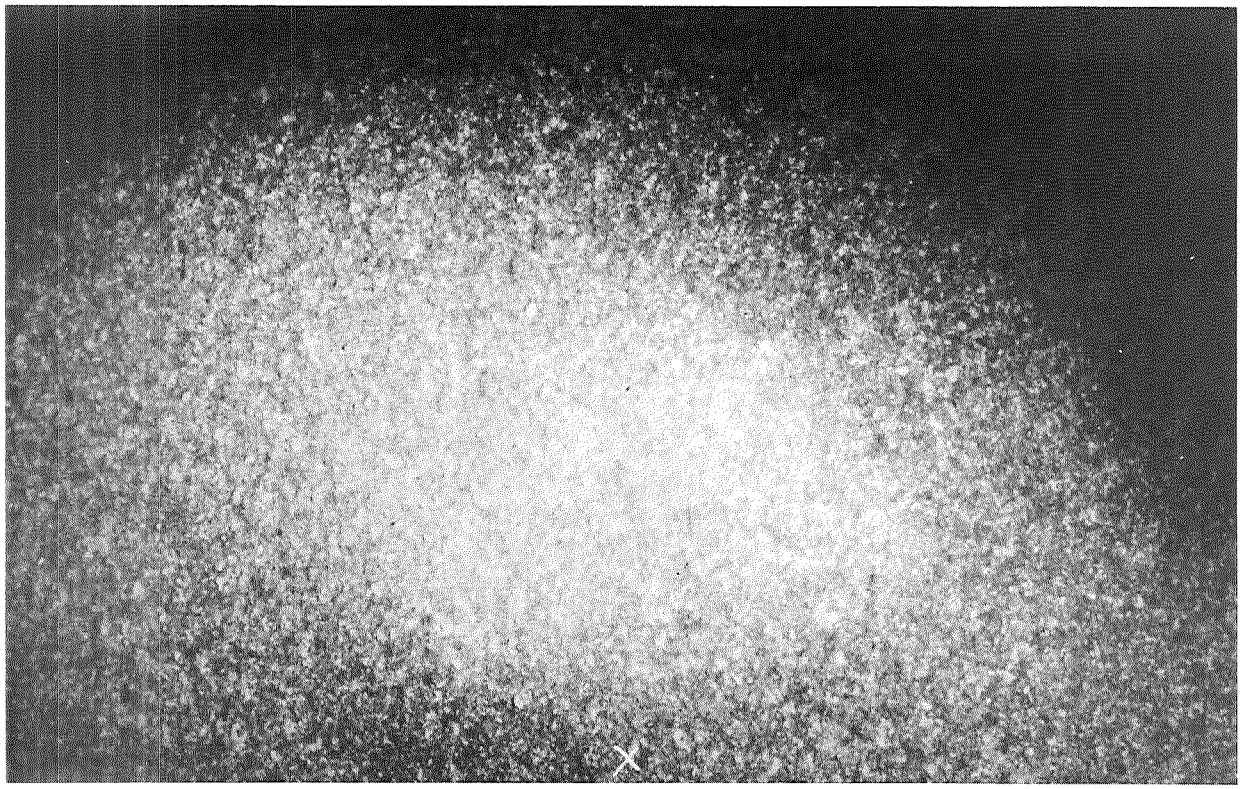

Figure 27. Aluminum Metallided System After 200 Hours Static Oxidation at 2000°F (1367°K) (C70052713, 10X).

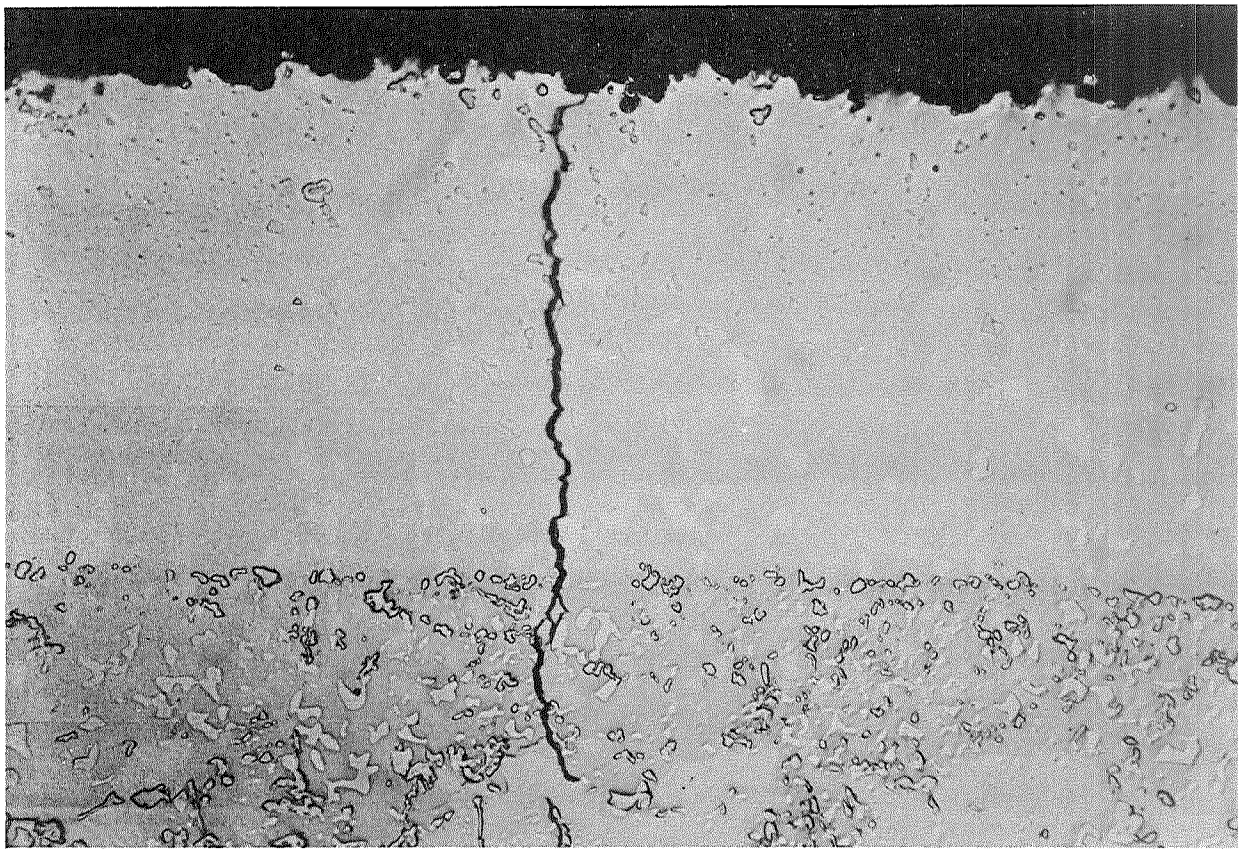

Figure 28. Aluminum Metallided System on NASA/TRW VI-A After 200 Hours Static Oxidation at 2000°F (1367°K) (F 6006, 500X, Unetched).

A. Impacted Surface

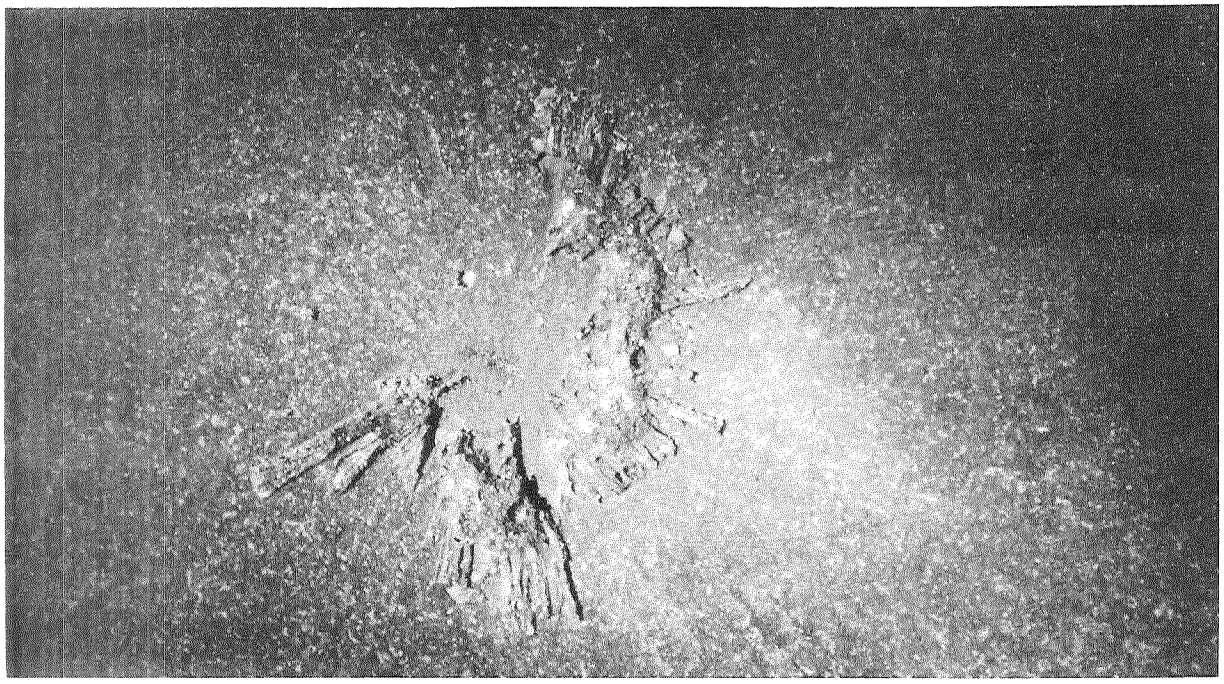

B. Surface Opposite Impact

Figure 29. Room Temperature Ballistically-Impacted Aluminum Metallided System After 200 Hours Static Oxidation at 2000°F (1367°K) (C70052715 Lower, C70052716 Upper, 10X).

Metallided Element Al and Ni Base

Substrate Elements

Substrate Elements

EBS

Ni

Ta

Co

Mo

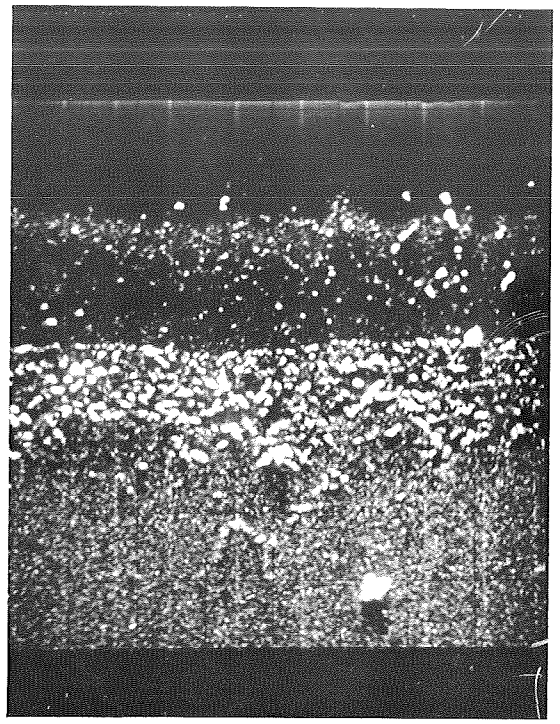

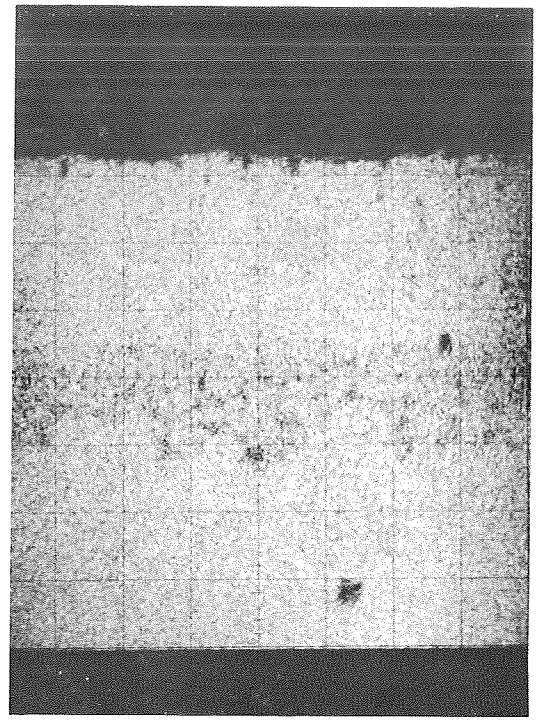

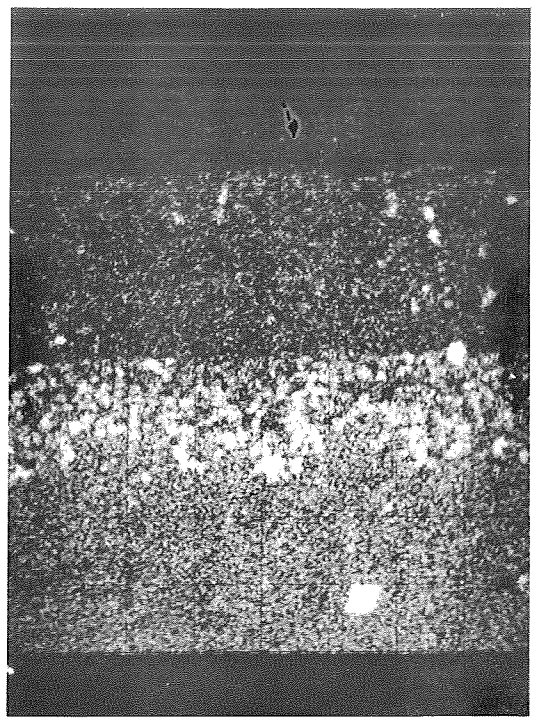

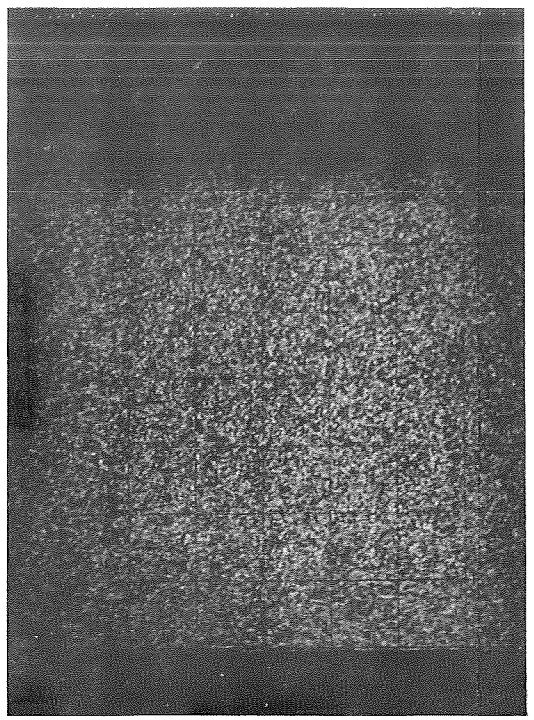

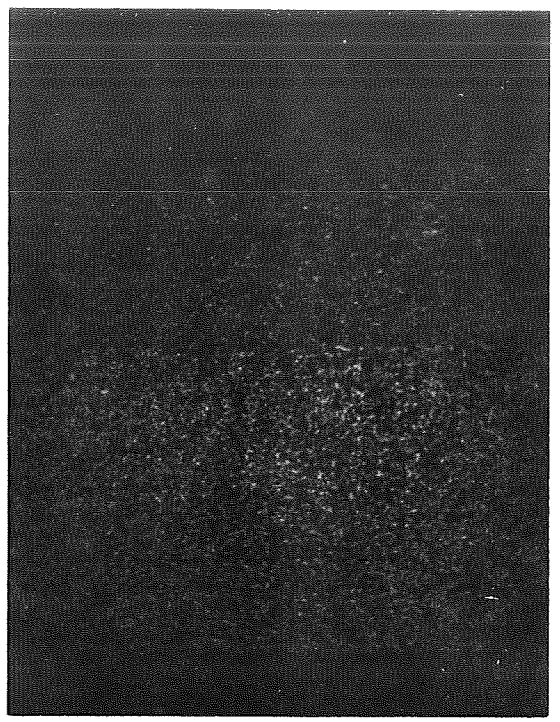

Al

Cr

W

Ti

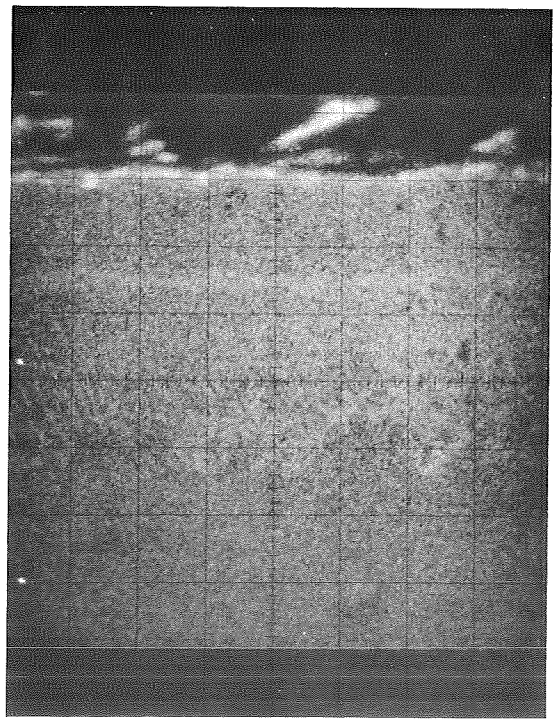

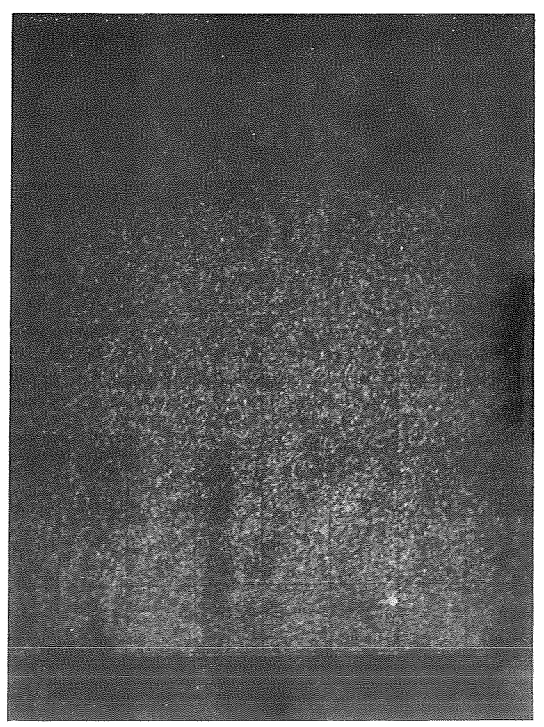

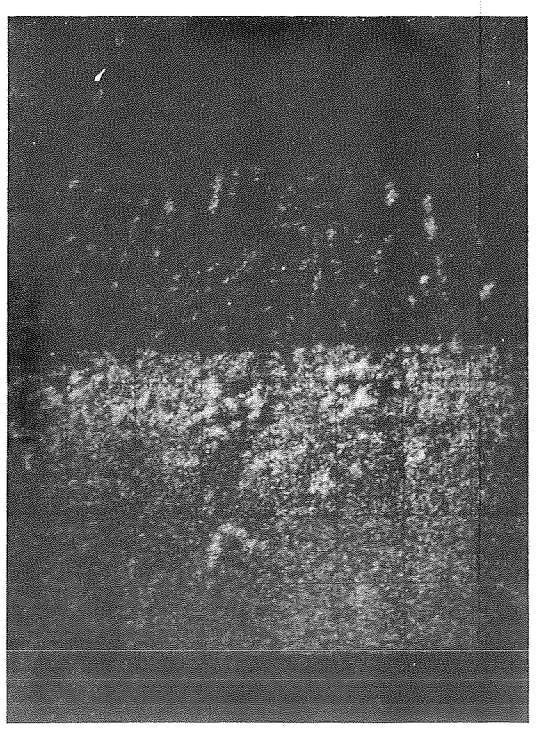

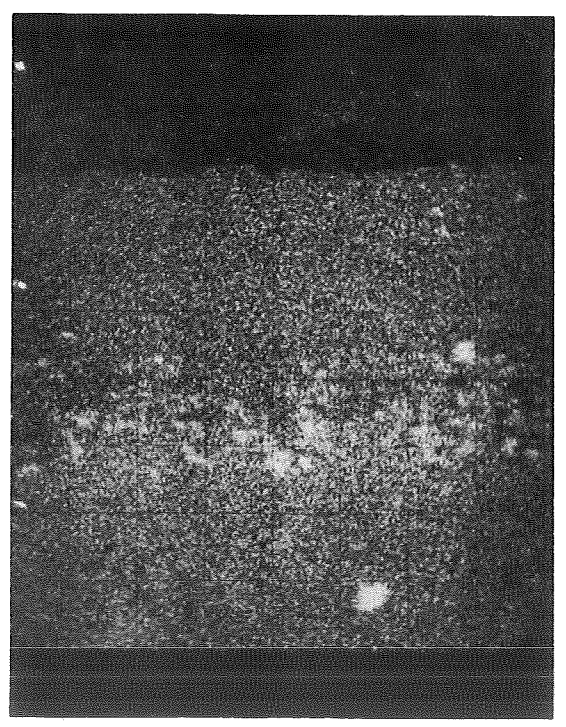

Figure 30. Microprobe Scans of Al Metallided NASA/TRW VI-A Showing Metallided Element and Ni Base After 200 Hours Static Oxidation at 2000°F (1367°K) (E 4701, 360X).

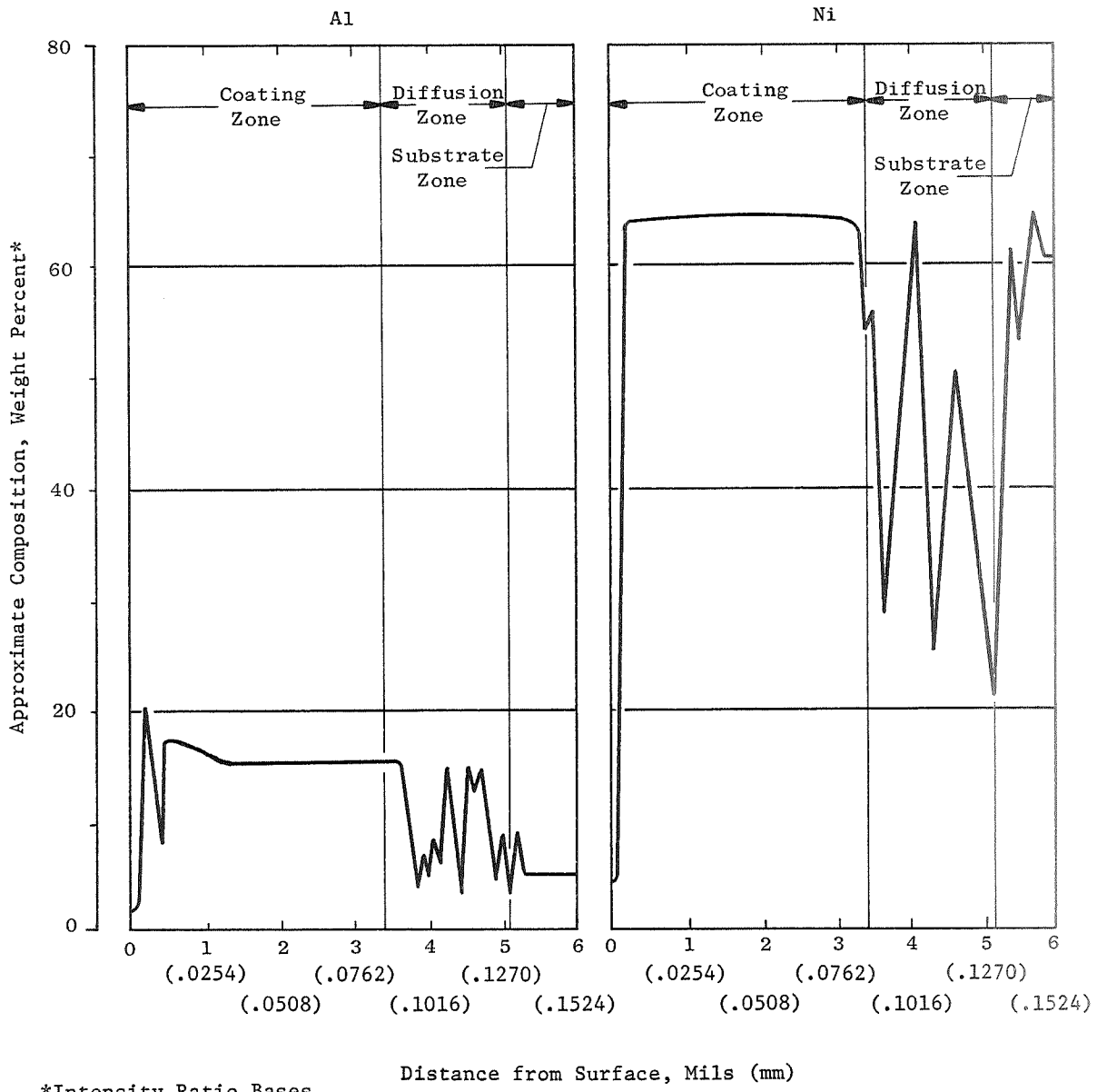

*Intensity Ratio Bases

Ni - NASA/TRW VI-A alloy
Al - NASA/TRW VI-A alloy and pure metal

Figure 31. Microprobe Trace of Al Metallided System on NASA/TRW VI-A After 200 Hours Static Oxidation at 2000°F (1367°K) (E 4701).

interdiffusion zone shows depressions of Ni which effect is also apparent as Ni-lean areas in the Ni EBS scan.

EBS scans of the principal elements show these phases concentrated in the intermediate zone to be the Ta-Ti and Ta-W solid solution compounds. These phases are also present in the primary diffused coating zone. Co and Cr appear uniformly distributed except for the outermost Al-rich layer. Mo shows a concentration in the intermediate layer and sparse but fairly uniform distribution in the primary coating.

3.5 DYNAMIC OXIDATION TESTS

3.5.1 Test Procedure

Dynamic oxidation tests were performed in a natural-gas-fired flame tunnel facility having a gas velocity of 0.05 Mach at 2000°F (1367°K). The test sequence was as follows:

1. Accumulate 100 hours at 2000°F (1367°K) with a thermal cycle by air-blast quenching to black heat for 3 minutes every hour and weigh after every 20 cycles.

2. Accumulate 900 additional hours unless coating failure occurs first at 2000°F (1367°K) with thermal-cycle quenching every hour and weigh after every 100 cycles.

Two specimens of each of the coatings Mn + Cr, Al + Y, Ta + Al (all on NASA/TWR VI-A) and CODEP on IN-100 were tested as shown in Table XI. The average weight change data are plotted in Figure 32.

Table XI. 2000°F (1367°K) Dynamic Oxidation Test Results.

	System	Metallide No.	Total Test Time, hrs	Total Weight Change, mg/cm^2
1)	Mn + Cr	130-3/157-5	20	- 7.82
		130-2/164-2	20	-12.29
3)	Al + Y	174-4/177-2	600	- 0.83
		176-1/179-4	600	- 2.09
4)	Ta + Al	122-6/125-4	600	+ 0.24
		122-4/125-3	600	- 2.14
7)	CODEP on	-	600	- 0.43
	IN-100	-	600	- 0.24

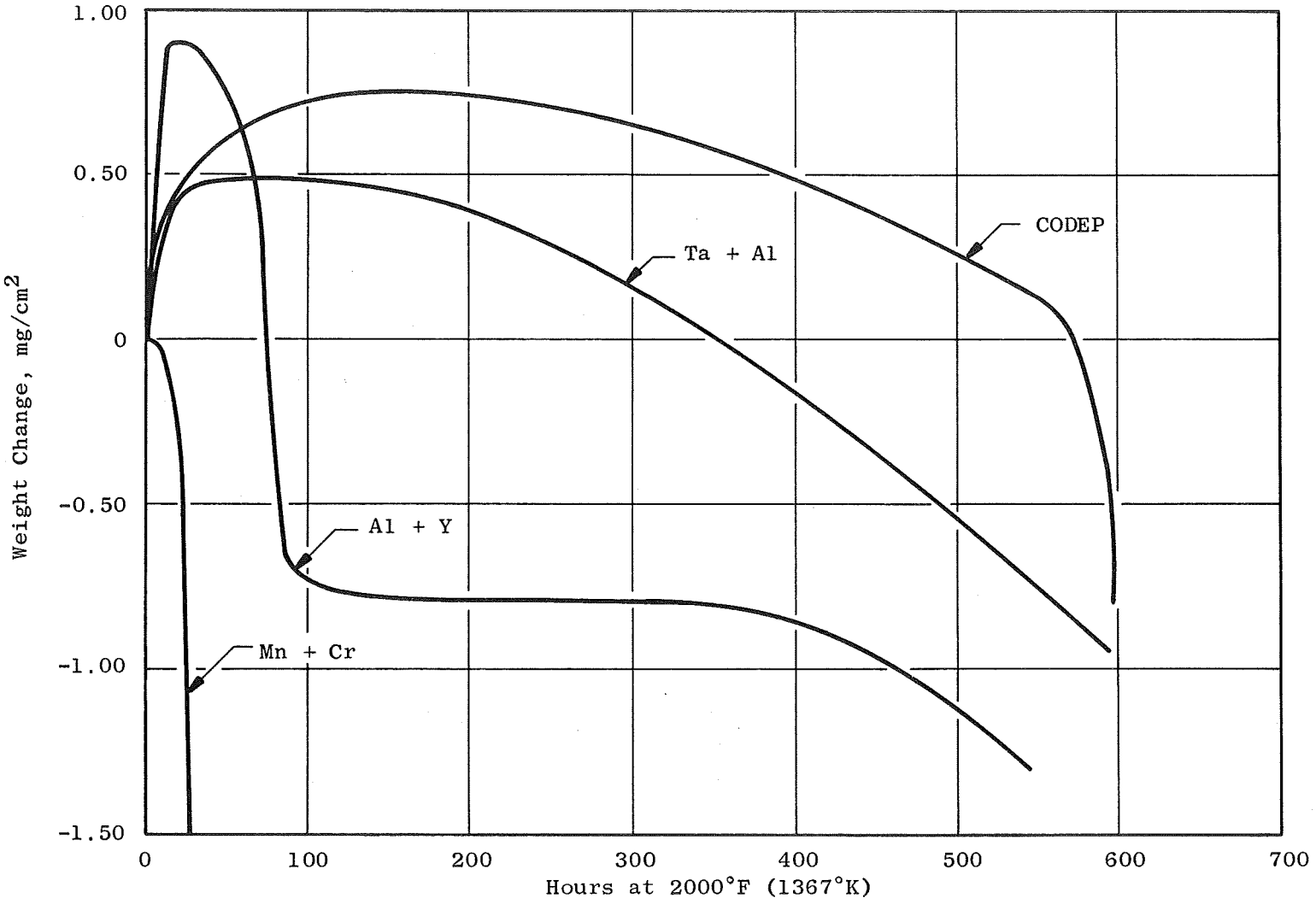

Figure 32. Dynamic Flame Tunnel Oxidation Test Results for Sequentially-Metallided, Dual-Element Coating Systems on NASA/TRW VI-A and CODEP-Coated IN-100. Specimens Thermal Cycled by Air Blast to 1000°F (811°K), Weighed Every 20 Cycles During the First 100 Hours, Then Weighed Every 100 Cycles During Test Duration.

3.5.2 Mn + Cr

Two specimens of the Mn + Cr coating were tested as-coated and failed by excessive spalling within 20 hours at 2000°F (1367°K). These specimens had not received the 1-hour, 2200°F (1478°K) postcoating vacuum heat treatment. Two additional specimens were then tested after heat treatment, but they also failed within 20 cycles. The specimens were similar in appearance to the statically-tested group described previously in Section 3.4.2 (static oxidation testing).

Figure 33 shows a typical metallographic section of the system after test. The general structure consists of the primary diffused coating layer and the intermediate diffusion layer on the NASA/TRW VI-A substrate. Figure 34 is the microprobe EBS scans of the individual metallided and major substrate elements. Mn is in very low concentration and Cr in high concentration, similar to the distribution shown for the static oxidation specimen. X-ray diffraction revealed the presence of hexagonal Cr_2O_3 and cubic Mn_3O_4. The oxides were not in spinel form, based on observed "d" spacings.

The Ni scan reveals lean areas which appear to be Cr-rich particles in the intermediate layer. Neither Ta- nor W-rich phases were detected; although, Ti-rich phases are present. This is unusual based on other scans which have shown Ta-Ti and Ta-W solid solution phases.

3.5.3 Al + Y

Two specimens were tested in dynamic oxidation as indicated in Table XII. The results were shown in Figure 32. Weight change patterns were similar to those for the static oxidation specimens, showing an initial weight gain as the surface Y oxidized, and then a weight loss within 100 hours. Stability was indicated up to 400 hours and then weight loss began again.

Figure 35 illustrates the general microstructure; the corresponding electron microprobe scan photos are shown in Figure 36. The structure is characterized by surface oxidation with no areas of gross penetration. There were coating cracks as before, but fewer than observed in the static oxidation specimen, and none of the cracks was oxidized. Possibly the longer exposure time at 2000°F (1367°K) rendered the coating less resistive to internal stress.

The metallographic structure displays the "white", Al-depleted gamma phase of the Ni-Al system and the darker Ni-Al phase in the primary diffusion zone. The secondary or interdiffusion zone contains enriched phases of Ta-Ti, Ta-W, and Mo-W solid solutions. X-ray diffraction analysis showed trigonal α-Al_2O_3 as the dominant surface phase. No Y patterns or mixed oxides were evident.

3.5.4 Ta + Al

The weight change data for specimens of this system were contained in Figure 32. After an initial weight gain, the specimens underwent a gradual

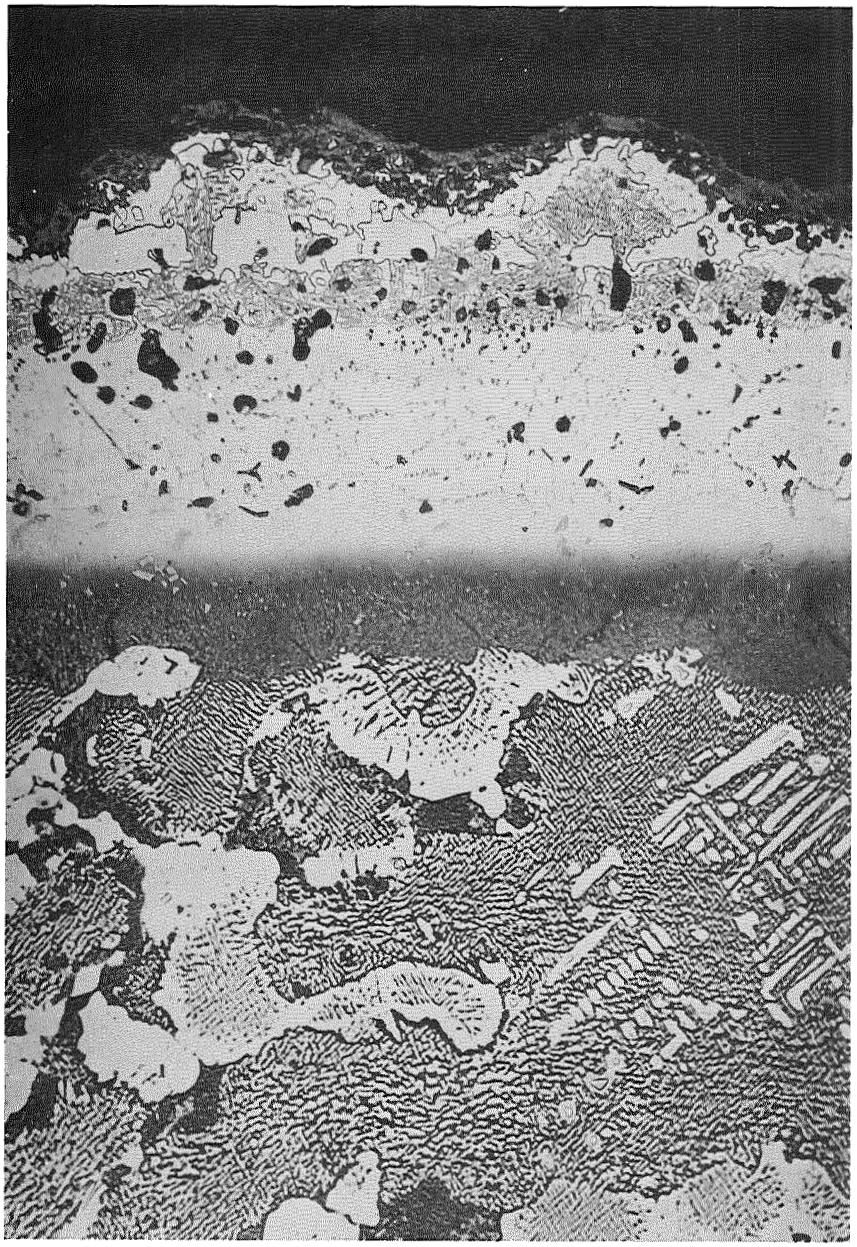

Figure 33. Mn + Cr Metallide System on NASA/TRW VI-A After 20 Hours Dynamic Oxidation at 2000°F (1367°K) (F 6023, 500X, TRW Etch).

Metallided Elements Mn + Cr and Ni Base

Substrate Elements

Substrate Elements

EBS

Ni

Ta

Co

Mo

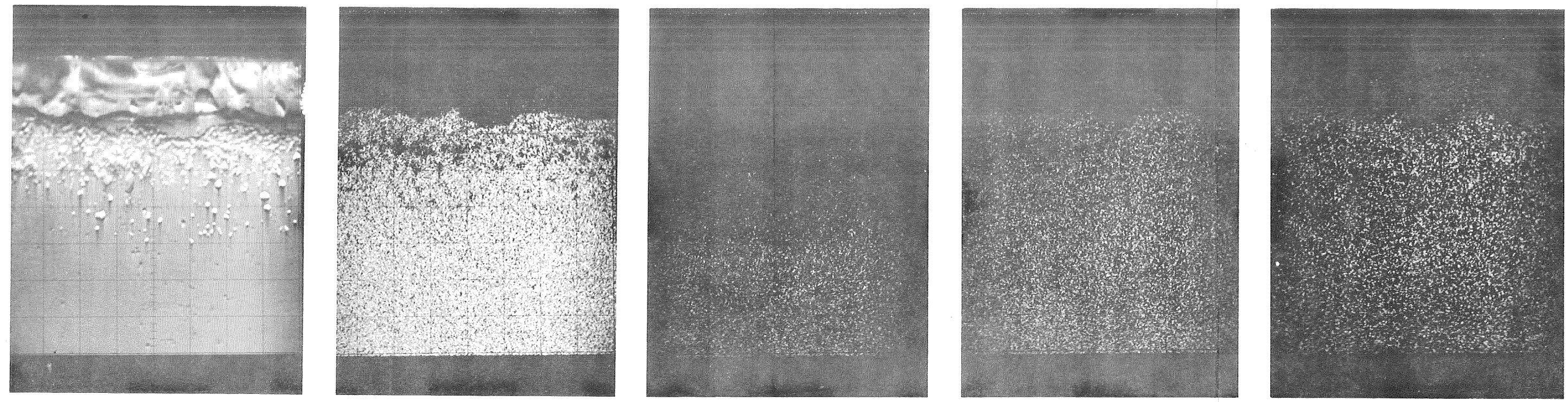

Mn

Cr

W

Al

Ti

Figure 34. Microprobe Scans of Mn + Cr Metallide System on NASA/TRW VI-A Showing Metallided Elements and Ni Base After 20 Hours Dynamic Oxidation at 2000°F (1367°K) (E 4933, 360X).

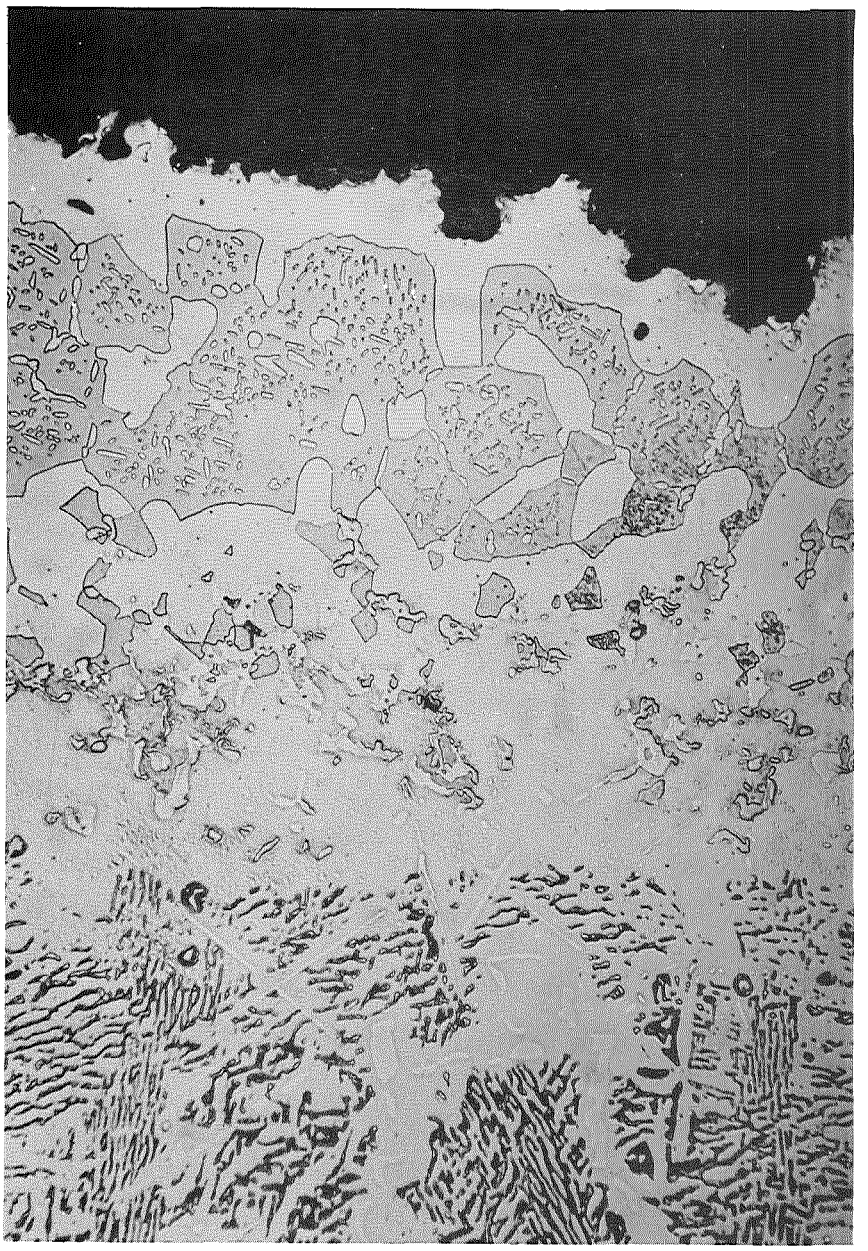

Figure 35. Al + Y Metallided System on NASA/TRW VI-A After 600 Hours Dynamic Oxidation at 2000°F (1367°K) (F 6019, 500X, TRW Etchant).

Metallided Elements Al + Y and Ni Base

Substrate Elements

Substrate Elements

EBS

Ni

Ta

Co

Mo

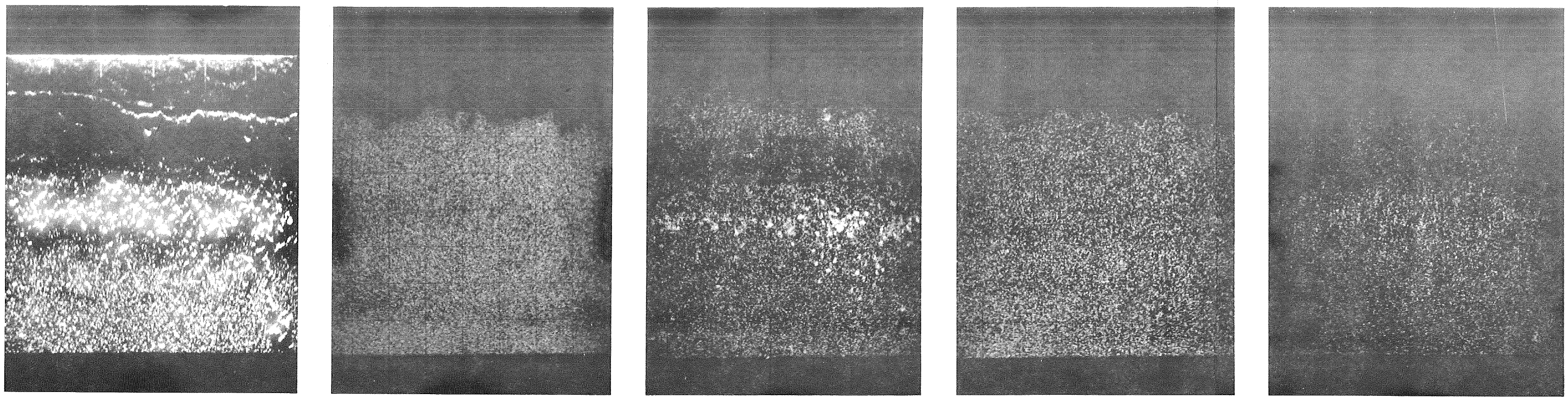

Al

Y

Cr

W

Ti

Figure 36. Microprobe Scans of Al + Y Metallided System on NASA/TRW VI-A Showing Metallided Elements and Ni Base After 600 Hours Dynamic Oxidation at 2000°F (1367°K) (E 4927, 360X).

weight loss during the 600-hour exposure. This was a contrast to the spalling and rapid weight change occasioned by the static oxidation tests. Figure 37 is a composite photomicrograph to show the deep interdiffusion of the metallided elements. The coating contained fine nonoxidized cracks after metallographic preparation.

Figure 38 is the microprobe EBS individual element scans. There are four distinct compositional bands in this structure:

(1) The outer or surface layer

(2) a primary diffusion zone

(3) a secondary diffusion zone

(4) an interdiffusion zone adjacent to the substrate

Enrichment of Ta and Al is seen in the surface oxide layer. The outer layer also contains all the major substrate elements. W appears in identical surface concentration as the Ta. The Ta, W, and Ti are present in identical phase patterns in the deep interdiffused zone, but Ti is more enriched in the secondary diffusion zone than the Ta or W.

The secondary zone shows Al enrichment and appears to be NiAl, while the white phase in the primary diffusion zone, depleted of Al, appears to be gamma phase.

Cr exhibits gradients not apparent in the other systems. It is present in the primary layer but is more concentrated in the secondary layer. Cr appears to occupy the network of intergranular phases in the secondary layer. An even higher concentration of Cr is shown in the interdiffusion zone. Mo was present in all the diffusion layers but was concentrated as discrete phase in the interdiffusion zone. X-ray diffraction analysis of the surface phases indicated a predominance of trigonal α-Al_2O_3. Minor indications of a possible TaO phase were revealed. No mixed oxides were indicated.

3.5.5 CODEP-Coated IN-100

The CODEP C-2 processed specimens exhibited relatively good stability through 550 thermal cycles then underwent a sharp loss at the final weighing, as was shown in Figure 32. The metallographic appearance of the coating after test is shown in Figure 39, and the electron microprobe EBS and individual element scans are shown in Figure 40.

Aluminum is shown to be concentrated in the outer oxide layer, also a concentration of Cr exists in a layer immediately below the Al_2O_3. The "white" phase in the photomicrograph is characteristic of gamma NiAl. Ti and Mo are shown as enriched indentical phases and in concentration in the dark phase band separating the white layer. The darker lowest diffusion band appears to have Cr and Mo concentrations and to be low in Ti. The white areas of the microstructures are rich in Ti and low in Mo and Cr.

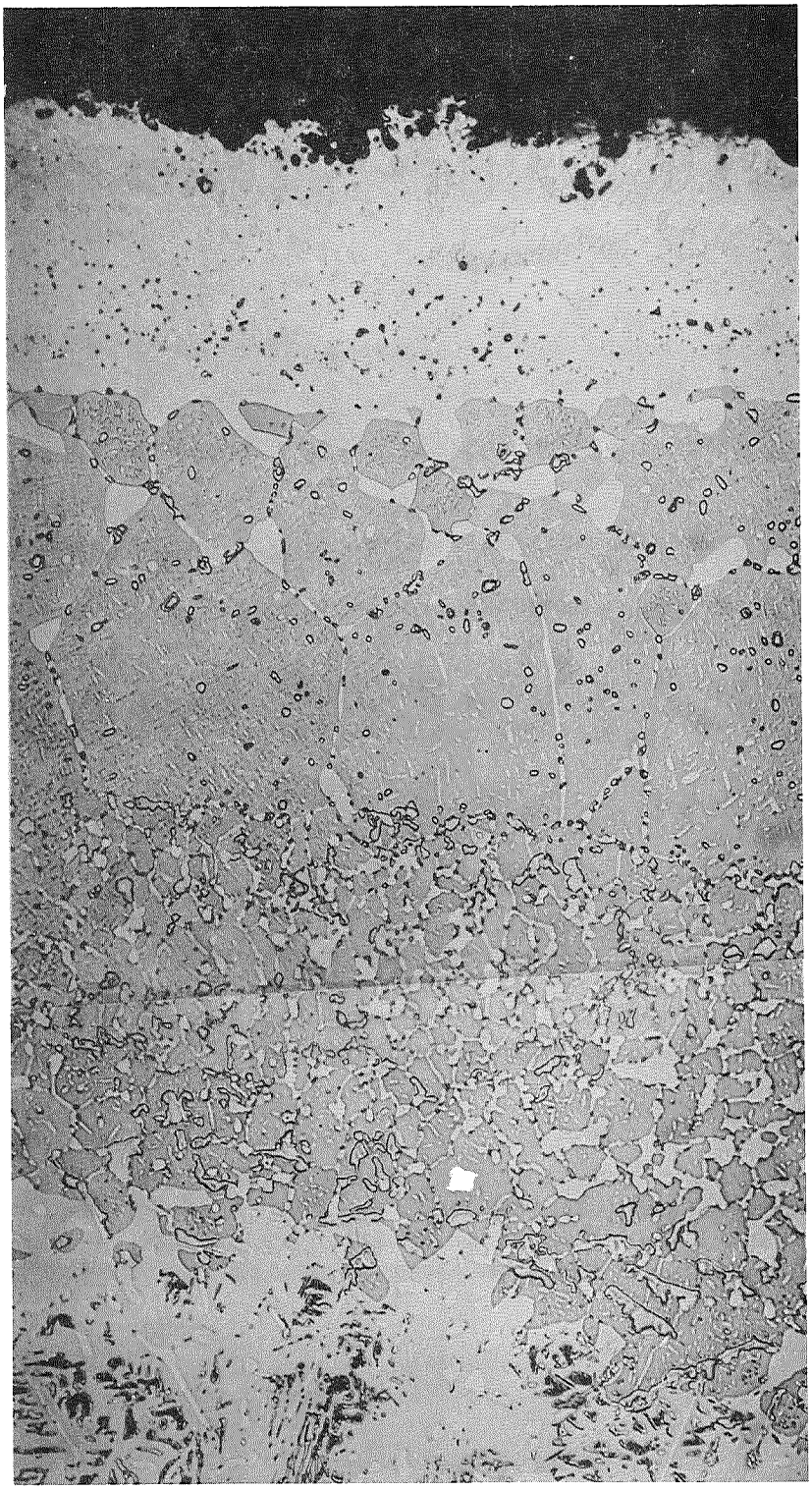

Figure 37. Ta + Al Metallided Systems on NASA/TRW VI-A After 600 Hours Dynamic Oxidation at 2000°F (1367°K) (F 6020, F 6021, 500X, TRW Etch).

Metallided Elements Ta + Al and Ni Base

EBS

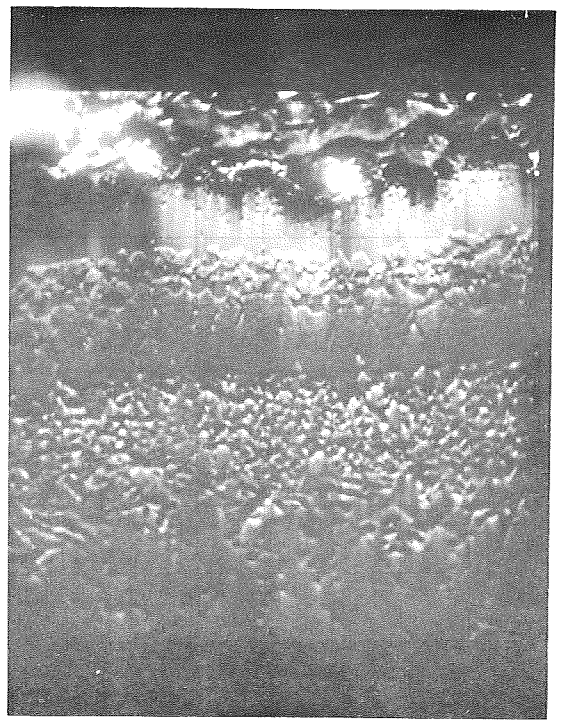

Ni

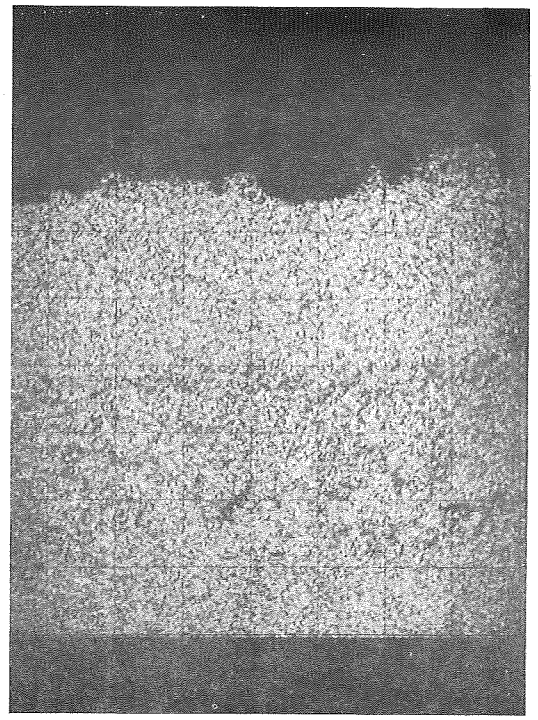

Ta

Al

Cr

W

Ti

Substrate Elements

Co

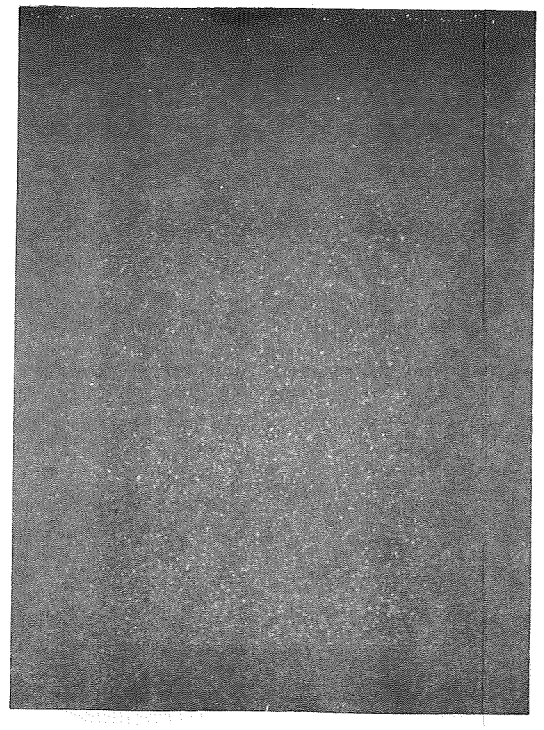

Substrate Elements

Mo

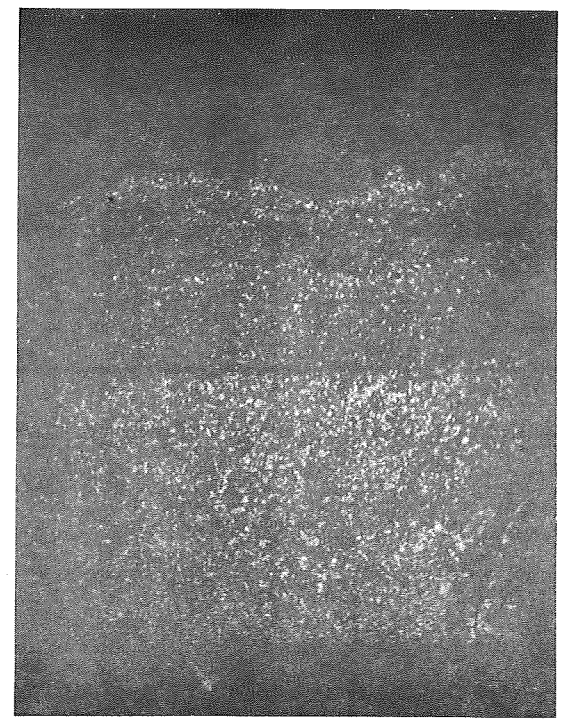

Figure 38. Microprobe Scans of TA + Al Metallided System on NASA/TRW VI-A Showing Metallided Elements and Ni Base After 600 Hours Dynamic Oxidation at 2000°F (1367°K) (E 4929, 360X).

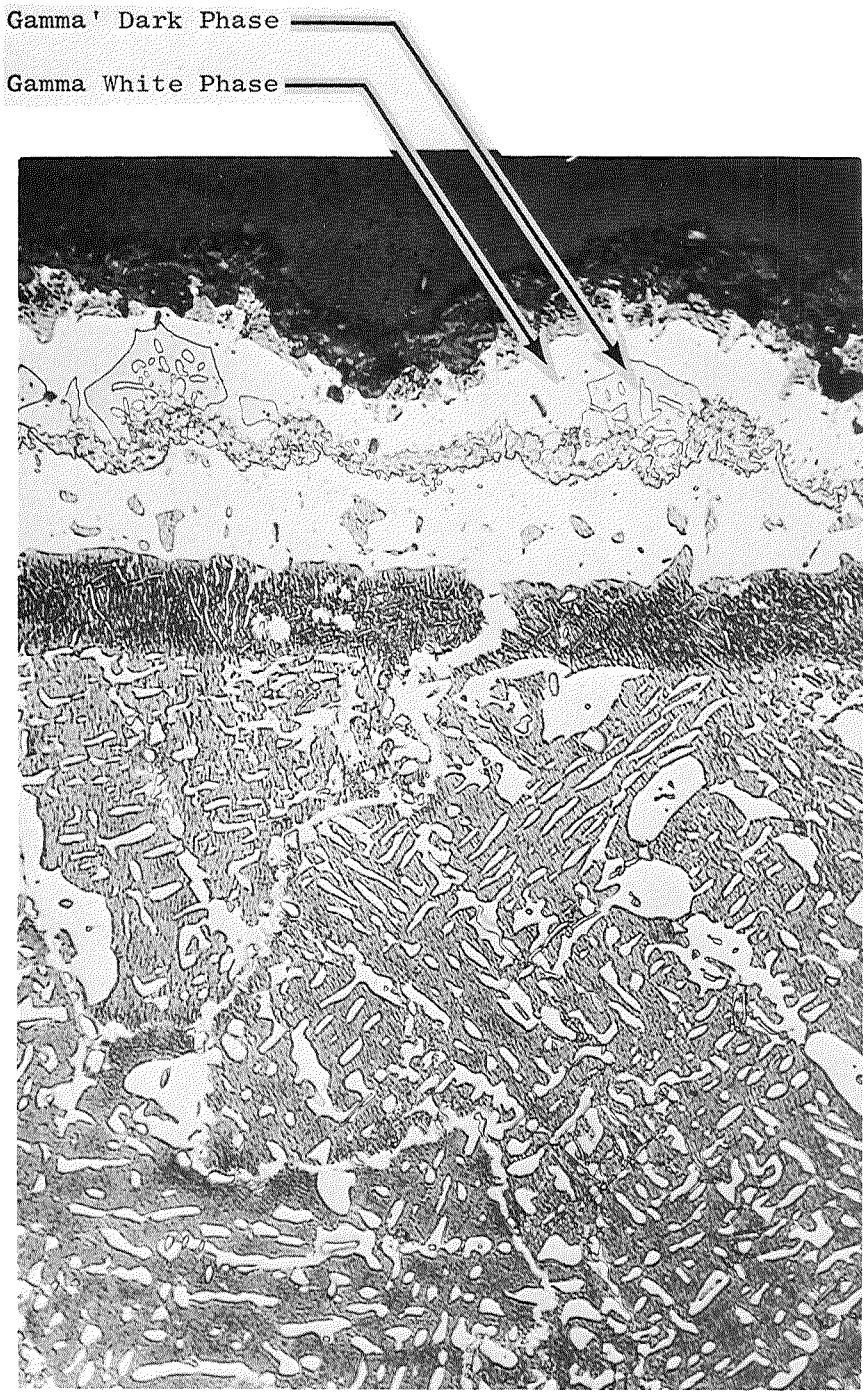

Figure 39. General Electric CODEP C-2 Pack-Type Aluminized Coating on IN-100 Alloy After 600 Hours Dynamic Oxidation at 2000°F (1367°K) (F 6022, 500X, TRW Etch).

Principal Additives and Ni Base

Substrate Elements

EBS

Ni

Cr

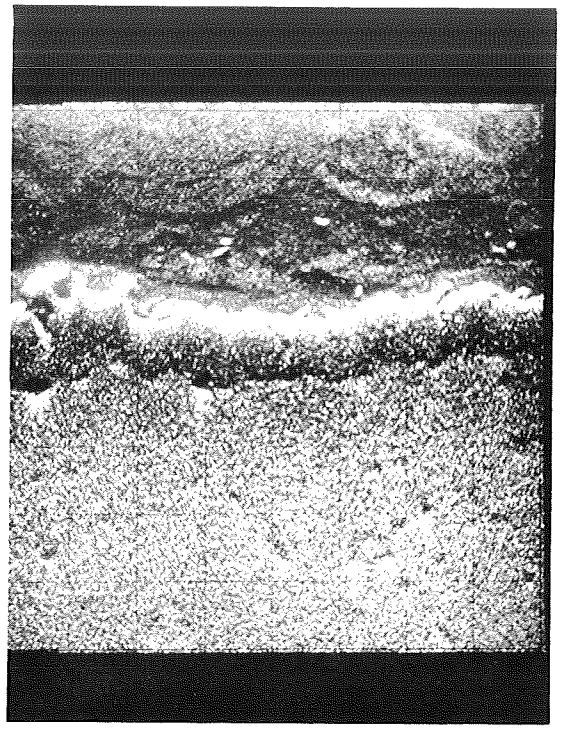

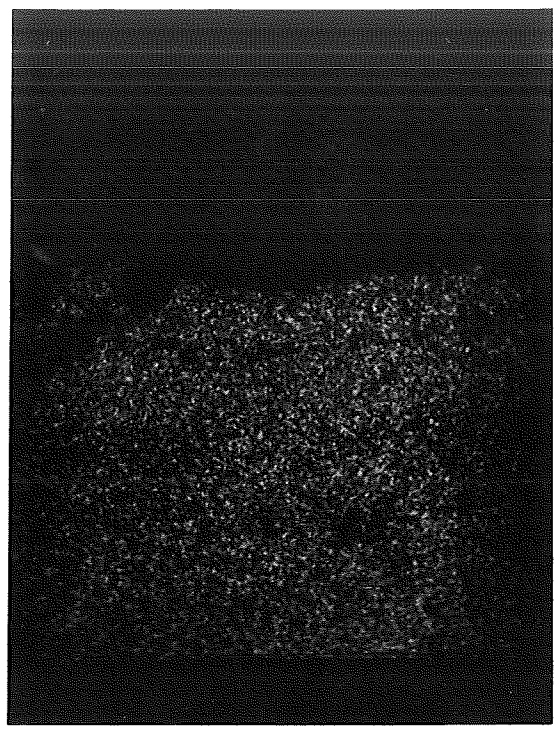

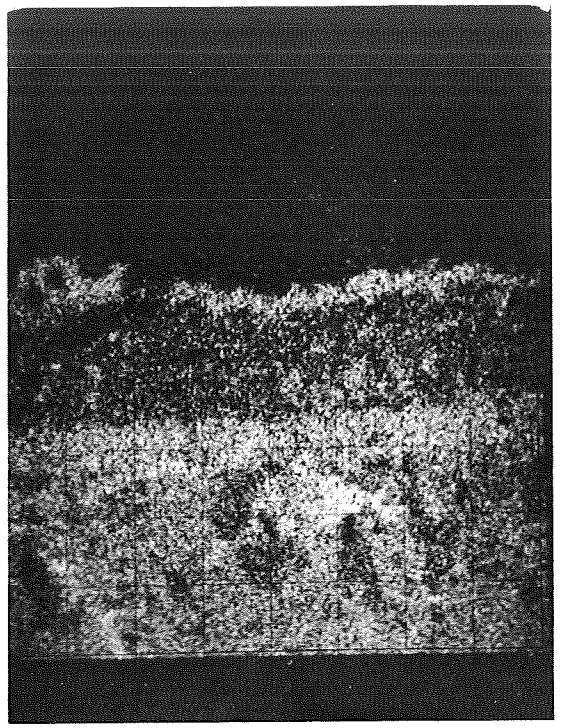

Al

Ti

Mo

Co

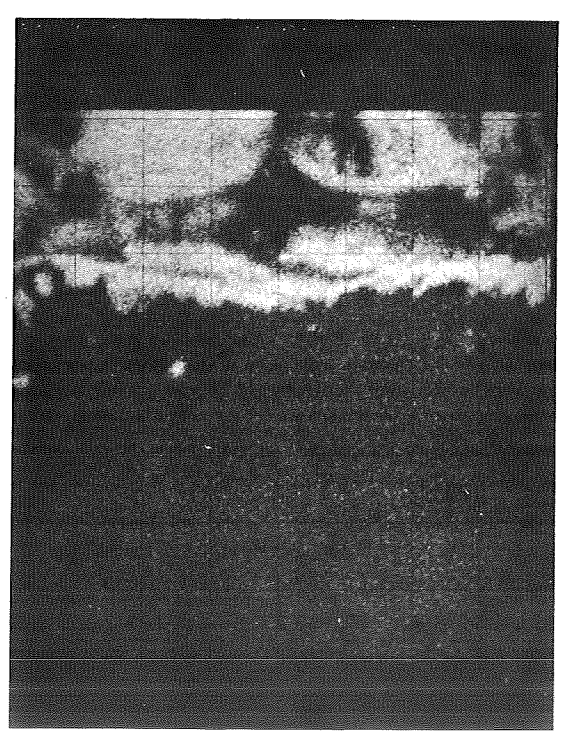

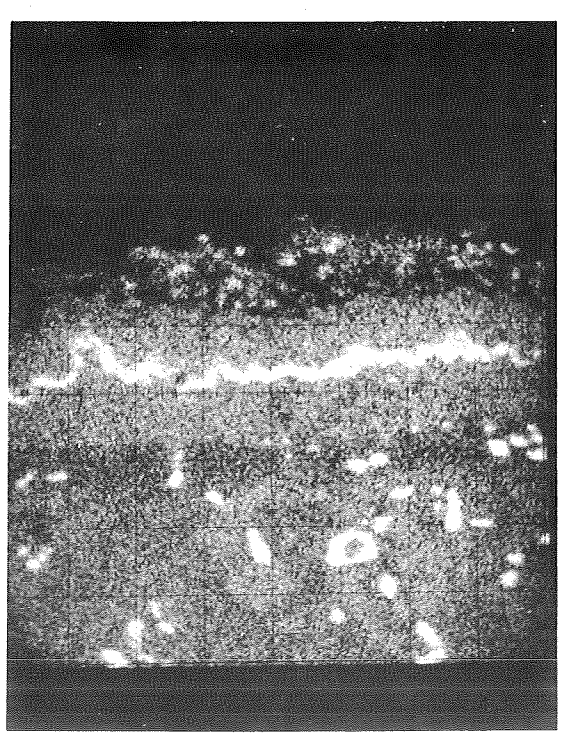

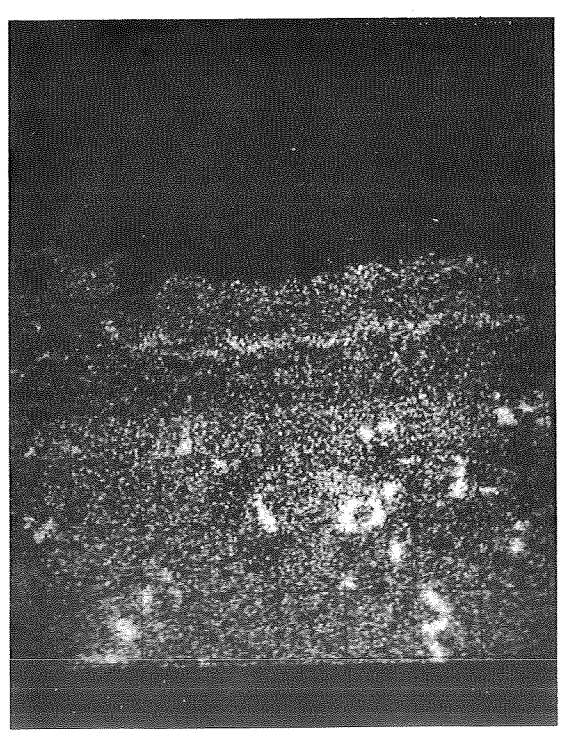

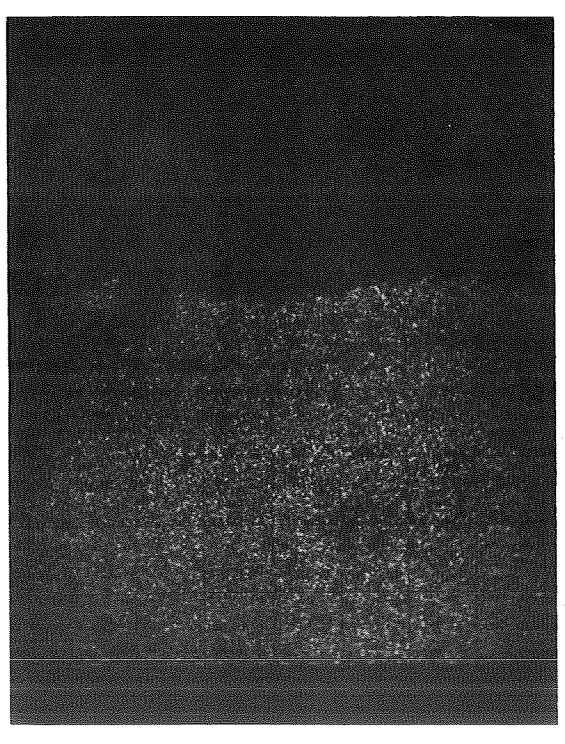

Figure 40. Microprobe Scans of CODEP C-2 on IN-100 Showing Principal Additives and Ni Base After 600 Hours Dynamic Oxidation at 2000°F (1367°K) (E 4931, 360X).

Furthermore, Ti appears as particles in the Al_2O_3 layer, as the result of TiO_2 particles in the original coating. X-ray diffraction confirmed the presence of α-Al_2O_3 and rutile TiO_2. Ni and Co are present through the structure except for the oxide layer and the Mo-Ti phase areas.

4.0 DISCUSSION

The progression from single-element metalliding to dual-element metalliding has proved to be more complicated than anticipated. Three types of problems appeared for two element processes: (1) the formation of low melting phases by three or more elements alloying in the surface region, (2) reaction with the bath of the first element deposited during metalliding of the second element, and (3) solid state diffusion reactions that prevented formation of the target coating chemistry or structure. These have combined to limit the number of coating systems that were good enough to test.

The formation of a low melting phase was clearly responsible for the failure of the Y + Zr system. A Ni-Zr eutectic, in equilibrium at 1760°F (1235°K), may have been found in the diffused coating and had its eutectic temperature depressed by alloying from other NASA/TRW VI-A ingredients to form the observed molten state in the yttriding process. The state of the art does not yet allow before-hand prediction of when melting will occur at bath temperatures.

Attempts to deposit yttrium first invariably produced reactions between the deposited yttrium layer and the subsequent fluoride baths for chromiding and aluminiding. The high affinity of Y for F and perhaps the formation of YF_3 in the bath are to be expected on the basis of the very low free energy of formation of YF_3. By reversing the order of metalliding, that is by depositing Cr or Al first and then Y, a two-element coating could be produced. In the case of the Mn + Cr system, the loss of Mn in the chromiding step, as measured by weight changes and probe analyses, demonstrated a reaction or dissolution of the Mn deposit with the bath. As a result, the desired Mn level of 1% and Cr level of 10-25% could not be achieved.

The complexity of diffusion reactions due to the presence of so many elements, from both the two coating metals and the alloy ingredients of NASA/TRW VI-A, also had ramifications. In the Mn + Cr system porosity developed, probably as a result of Kirkendall effects. Also, the inward diffusion of large amounts of Cr produced new phases with Ni and probably with Ta (and may also have changed the solubility of other base alloy elements, e.g., Al) so as to alter its distribution. The solubility effect is typical of most diffusion type coatings. The diffusion penetration of Y into aluminided base alloy seems to have been restricted, as was the diffusion penetration of Al into the tantalided base alloy. Very high Ta compositions were reached in some parts of the coating, leading one to consider that thermal expansion mismatch of the layers may have contributed to the spalling that occurred in cyclic oxidation exposure. Thus, attainment of desired chemical distributions and structures from coating processes alone already appear to bear some of the limiting features that were reflected in poor impact and oxidation behavior.

The degrading effects of oxidation exposure at 2000°F (1367°K) produced further changes in the coatings by loss of scale and by solid state diffusion. The Mn + Cr system failed to develop a stable, resistive spinel oxide, and the test samples lost weight quickly. The Al + Y system gained weight rapidly as an oxide glaze formed. When the glaze disappeared, the Y also was absent in probe scans, and then some protection resulted from what evidently was a Ni-Al system coating. In static oxidation, the Ta + Al spalled badly. This test used strong air-blast cooling to room temperature, and thermal strains were probably severe. Also, as noted, a thermal expansion mismatch among coating layers may have existed. In dynamic tests, thermal cycles were more gentle, and spalling did not occur. It permitted deep penetration of Ta and Al by diffusion and offered protection by what basically appears as a Ni-Al system coating with contained alloy phases.

The Al + Y, Ta + Al, Al and CODEP coatings originally were, or reached a stage where they behaved as, Ni-Al system coatings. The longest survivors in oxidation tests were essentially those coated originally with a plain Ni-Al system. Consequently, this exploration of dual-coating systems did not produce any improvement over aluminide state-of-the-art coatings.

5.0 SUMMARY OF RESULTS

Five sequentially-deposited dual-element coating systems were selected for metalliding parameter development and oxidation testing at 2000°F (1367°K). The initially-chosen systems plus a sixth, added when others were unsuccessful, are listed in Table XII.

Table XII. Metalliding Systems and Process Results.

System	Metallided Elements		Metalliding Results
	First	Second	
1	Mn	Cr	Feasible. Specimens prepared for oxidation test.
2	Y	Cr	Discontinued. Highly-active Y driven off during chromiding.
3a	Y	Al	Discontinued due to Y loss during aluminiding. See System 3b below.
3b	Al	Y	Feasible. Specimens prepared for oxidation test.
4	Ta	Al	Feasible. Oxidation tested.
5	Y	Zr	Discontinued. Zr addition too slow.
6	Al	---	Feasible. Oxidation tested.

Successfully-metallided coatings were subjected to ballistic-impact adherence at room temperature and 1900°F (1310°K). Only the Mn + Cr system did not exhibit spalling at room temperature. None exhibited spalling at elevated temperature. However, during subsequent oxidation, all impacted specimens developed oxidation attack and spalling on the back side of the impact side.

Systems 1, 3, 4, and 6 were evaluated for 200 hours in static air furnace oxidation at 2000°F (1367°K), including thermal cycles to room temperature every two hours except for 16-hour holds overnight after the first 24 hours of testing. Results are plotted in Figure 41. The Mn + Cr and Ta + Al systems failed rapidly by spalling. The Al + Y system exhibited far better stabilization after initially shedding the oxidized Y layer. The Al-metallided system was the most stable, showing only small weight losses during the 200-hour exposure.

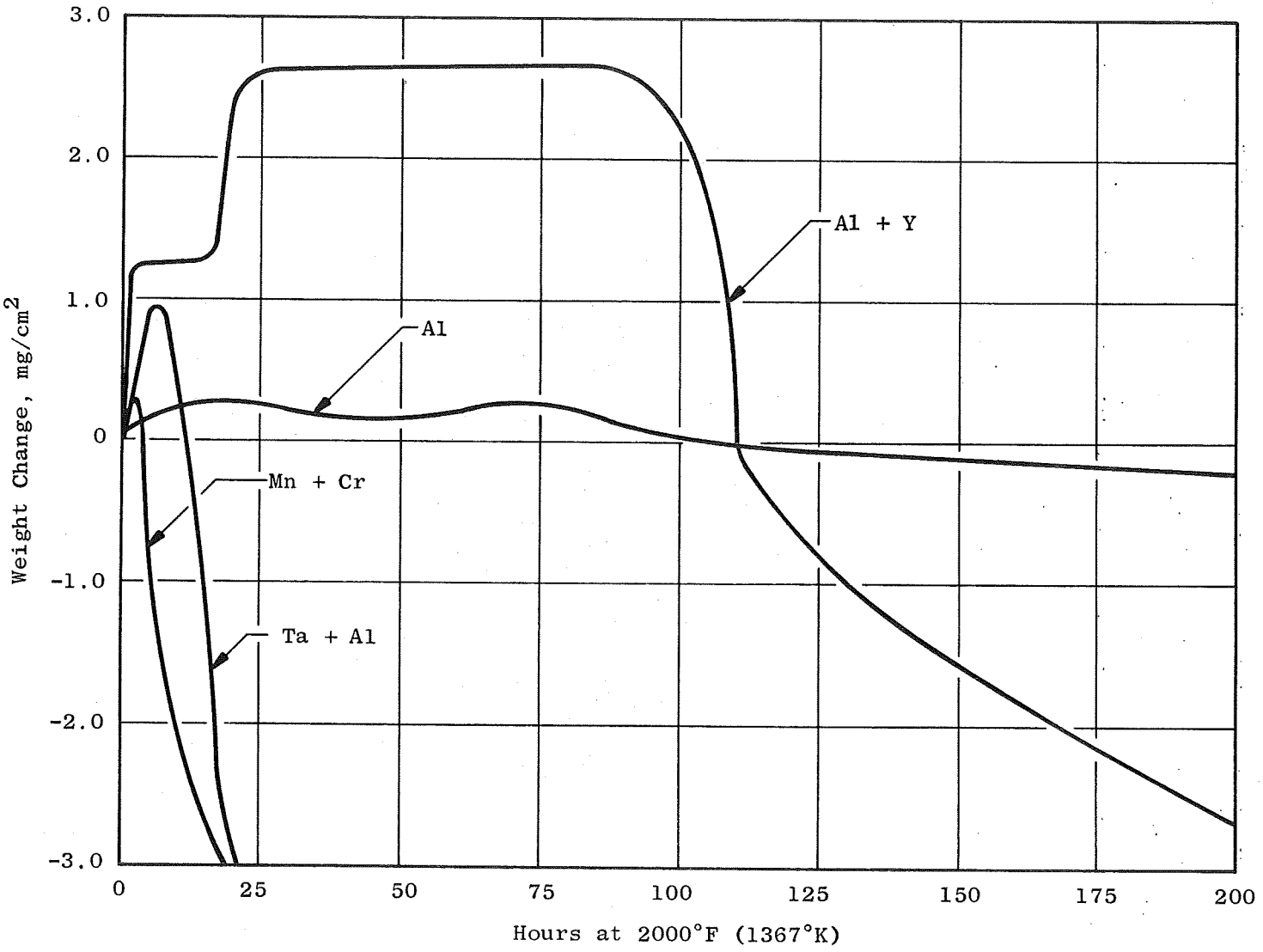

Figure 41. Static Air Furnace Oxidation Test Results for Sequentially-Metallided, Dual-Element Coating Systems on NASA/TRW VI-A. Specimens Thermal Cycled and Weighed Every Two Hours During First Twenty-Four Hours, Then in Patterns of Three 2-Hour Holds and One 16-Hour Hold During the Test Duration.

Systems 1, 3, and 4 were also evaluated for 600 hours in dynamic flame tunnel oxidation (Mach 0.05) at 2000°F (1367°K). Specimens were thermal cycled every hour, but were only cooled to 1000°F (811°K) each hour, which significantly minimized spalling. The results are shown in Figure 42. The Mn + Cr system again failed rapidly. However, in contrast to the static oxidation results, Ta + Al exhibited a gradual but persistent weight loss. The Al + Y system demonstrated the same stabilization pattern after losing the Y as in static oxidation, but (after about 400 hours) again underwent a steady weight loss.

CODEP coating on IN-100, introduced as a standard, showed good stability to nearly 600 hours and then failed rapidly.

Spalling of the Mn + Cr and Ta + Al systems precluded meaningful posttest analyses. The primary aluminided layer of the Al + Y and the Al systems showed the presence of an aluminided-depleted gamma phase which accompanies coating failure. The Y layer did not interact to stabilize the Al + Y system.

Although the metalliding of TRW VI-A alloy with certain duplex-element systems was feasible, outstanding oxidation protection was not achieved. Additional study would be required to determine the benefit of postcoating heat treatments and compositional variations for achieving the postulated spinel and stabilized surface alloys for the desired oxidation resistance.

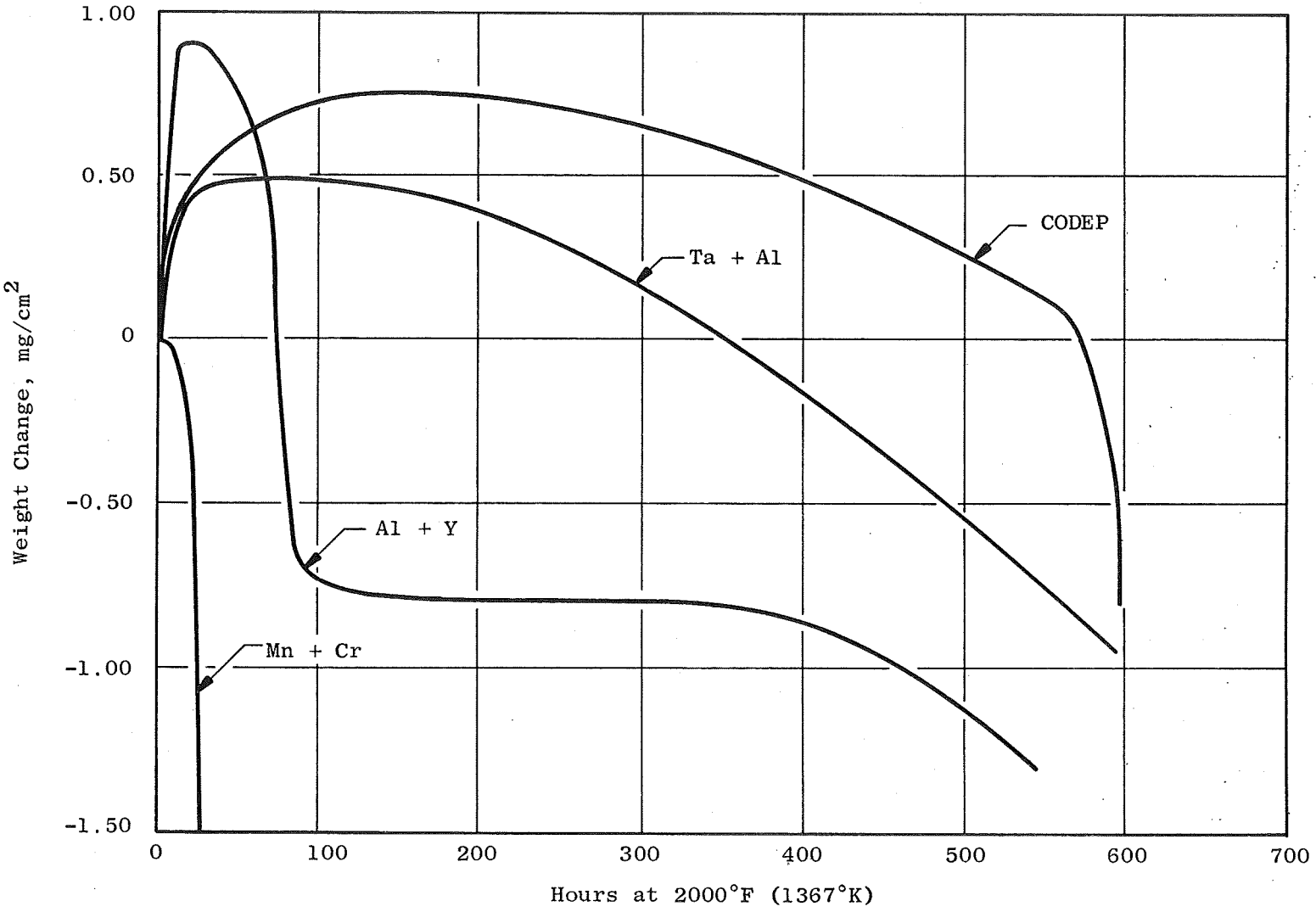

Figure 42. Dynamic Flame Tunnel Oxidation Test Results for Sequentially-Metallided, Dual-Element Coating Systems on NASA/TRW VI-A and CODEP-Coated IN-100. Specimens Thermal Cycled by Air Blast to 1000°F (811°K), Weighed Every 20 Cycles During the First 100 Hours, Then Weighed Every 100 Cycles During Test Duration.